8524

CONTRACTOR REPORT

SAND89—7143
Unlimited Release
UC—721

RS-8232-2/ 70987

Theory and Verification for the GRASP II Code for Adjoint-Sensitivity Analysis of Steady-State and Transient Ground-Water Flow

8232-2//070987,

00000001 -

Banda S. RamaRao, Mark Reeves
INTERA Inc.
6850 Austin Center Blvd., Suite 300
Austin, Texas 78731

Prepared by Sandia National Laboratories Albuquerque, New Mexico 87185 and Livermore, California 94550 for the United States Department of Energy under Contract DE-AC04-76DP00789

Printed October 1990

Available to DOE and DOE contractors from
Office of Scientific and Technical Information
PO Box 62
Oak Ridge, TN 37831

Prices available from (615) 576-8401, FTS 626-8401

Available to the public from
National Technical Information Service
US Department of Commerce
5285 Port Royal Rd
Springfield, VA 22161

NTIS price codes
Printed copy: A05
Microfiche copy: A01

SAND89-7143
Unlimited Release
Printed October 1990

Distribution
Category UC-721

THEORY AND VERIFICATION FOR THE GRASP II CODE FOR ADJOINT-SENSITIVITY ANALYSIS OF STEADY-STATE AND TRANSIENT GROUND-WATER FLOW*

Banda S. RamaRao and Mark Reeves
INTERA Inc.
6850 Austin Center Blvd., Suite 300
Austin, Texas 78731

ABSTRACT

Calibration of a numerical model of the regional ground-water flow in the Culebra dolomite at the Waste Isolation Pilot Plant in southeastern New Mexico, has been performed by an iterative parameter-fitting procedure. Parameterization has been secured by choosing to assign the transmissivity values at a limited number of selected locations, designated as pilot points. The transmissivity distribution in the model is derived by kriging the combined pool of measured and pilot-point transmissivities. Iterating on the twin steps of sequentially adding additional pilot point(s) and kriging leads to the model of required accuracy, as judged by a weighted least-square-error objective function. At the end of calibration, it must be ensured that the correlation structure of the measured transmissivities is broadly preserved by the pilot-point transmissivities. Adjoint-sensitivity analysis of the model has been coupled with kriging to provide objectively the optimal location of the pilot points during an iteration. The pilot-point transmissivities have been adjusted by modeler's judgement incorporating information, where available, on local geologic conditions and large-scale hydraulic interference tests, in order to minimize the objective function.

* The work described in this report was done for Sandia National Laboratories under Contract No. 32-1025.

Adjoint methodology offers an efficient algorithm for calculation of the required parameter sensitivities. It separates the analysis into two distinct stages, with the first one related exclusively to the objective function, and the second one exclusively to the parameter of investigation, with the adjoint-state function from the first stage providing the link between the two stages. Implementing this philosophy, the equations of the adjoint sensitivities have been derived, keeping the partial variations with respect to pressure and parameters distinct. The adjoint-state function is interpreted to be an impulse-source response function in the transient state and a unit-source-rate influence function in the steady state. A three-dimensional finite-difference code, called GRASP II, has been built to implement the adjoint-sensitivity analysis, offering a wide range of options in objective functions and sensitivity parameters. The code has been extensively verified, by comparing the results with the sensitivity coefficients derived analytically and with those from a perturbation approach.

In this report, the theory and development of adjoint-sensitivity analysis and the verification of the numerical code are treated. A case study for the application of this coupled kriging-and-adjoint-sensitivity approach to calibration of the model for the site mentioned is presented in LaVenue et al (1990). The application demonstrates the usefulness of the present approach to calibration, particularly while handling a combination of the steady-state and transient head data.

ACKNOWLEDGEMENT

The authors are grateful to Richard L. Beauheim of the Sandia National Laboratories for his critical review of the manuscript. The authors thankfully acknowledge the contributions of John F. Pickens and Marsh LaVenue, with stimulating discussions during the course of this work.

CONTENTS

CONTENTS (Continued)

FIGURES

TABLES

INTRODUCTION

Numerical models are constructed to develop an understanding of and to predict the future states of a complex ground-water system. A necessary first step in such an exercise consists of the calibration of the numerical model, for which both direct and indirect approaches are available. This document considers an indirect approach, an iterative procedure, in which an appropriate distribution of the hydrogeologic parameters (such as the transmissivity and storativity) and the initial and boundary conditions, is sought to be established, to obtain the best fit of the model predictions with the historical observations, typically in a least-square sense. Model calibration, also referred to as parameter estimation, history-matching, or solution of the inverse problem, is a notoriously difficult but vitally important stage in the numerical modeling. The calibration procedure involves simulating with an initial trial estimate of the unknown parameters and then successively modifying the parameters and simulating until the desired convergence is achieved in the fit. Several variations of this approach, ranging from subjective trial-and-error procedures to fully automated inverse algorithms, are available (Yeh, 1986).

The number of parameter values (such as transmissivities) to be estimated in the calibration procedure must be reduced to a reasonable number and this procedure is called parameterization. This is usually accomplished by zonation, wherein the ground-water system is divided into a number of zones, in each of which the parameters are treated as constants. In this study, however, an alternative procedure of parameterization, using pilot points (de Marsily, 1984) is adopted. A pilot point is a location in the system, where the unknown parameters are sought to be estimated. From a limited number of assigned parameter values at the pilot points and the measured values of the parameters at well locations, the large number of parameter values required in the numerical model (in different grid blocks) are derived by suitable interpolation. Pilot points are chosen at locations where the model-fit criterion is most sensitive to the parameter variations.

Usually, prior to calibration of the ground-water model, information about the transmissivities at several locations in the site is obtained from pumping tests. In this study, kriging (de Marsily, 1986), an unbiased statistical linear-interpolation technique minimizing the variance of the estimation error, has been employed to derive the transmissivity distribution in the numerical model from the measurements in the transmissivity data base. Pilot points, which are added in each iteration, are defined by specifying a spatial location and assigning a transmissivity to that location. It is possible for the pilot-point data to be synthesized purely by the subjective judgement of the modeler. However, in this study, adjoint-sensitivity analysis of the numerical ground-water model has been coupled with kriging to yield objectively the optimal location of the pilot point. An appropriate minimization algorithm can be used to determine an estimate of the associated transmissivity. However, in this study it has been found expedient to use the modeler's best judgement to estimate the pilot-point transmissivity. This judgement incorporates information, where available, on local geologic conditions and large-scale hydraulic interference tests.

A separate report (LaVenue et al., 1990) presents the calibration efforts, using the combined kriging and adjoint-sensitivity approach presented here, on a numerical model of ground-water flow in the Culebra dolomite in the Rustler Formation at the Waste Isolation Pilot Plant (WIPP). The WIPP site is the location in southeastern New Mexico for a potential radioactive-waste repository being considered by the U.S. Department of Energy for isolation of defense transuranic wastes. A number of long-term pumping tests have been conducted at the WIPP site at different locations to obtain the transmissivities and the time-evolution of the pressure responses at the observation wells.

Figure 1 shows an example of a two-dimensional grid superimposed on a regional ground-water system, along with well locations. At each iteration, a number of candidate pilot-point locations are considered as shown in the pilot-point grid (Figure 1). The sensitivities of the least-square criterion function to the transmissivity 'data' at the pilot points

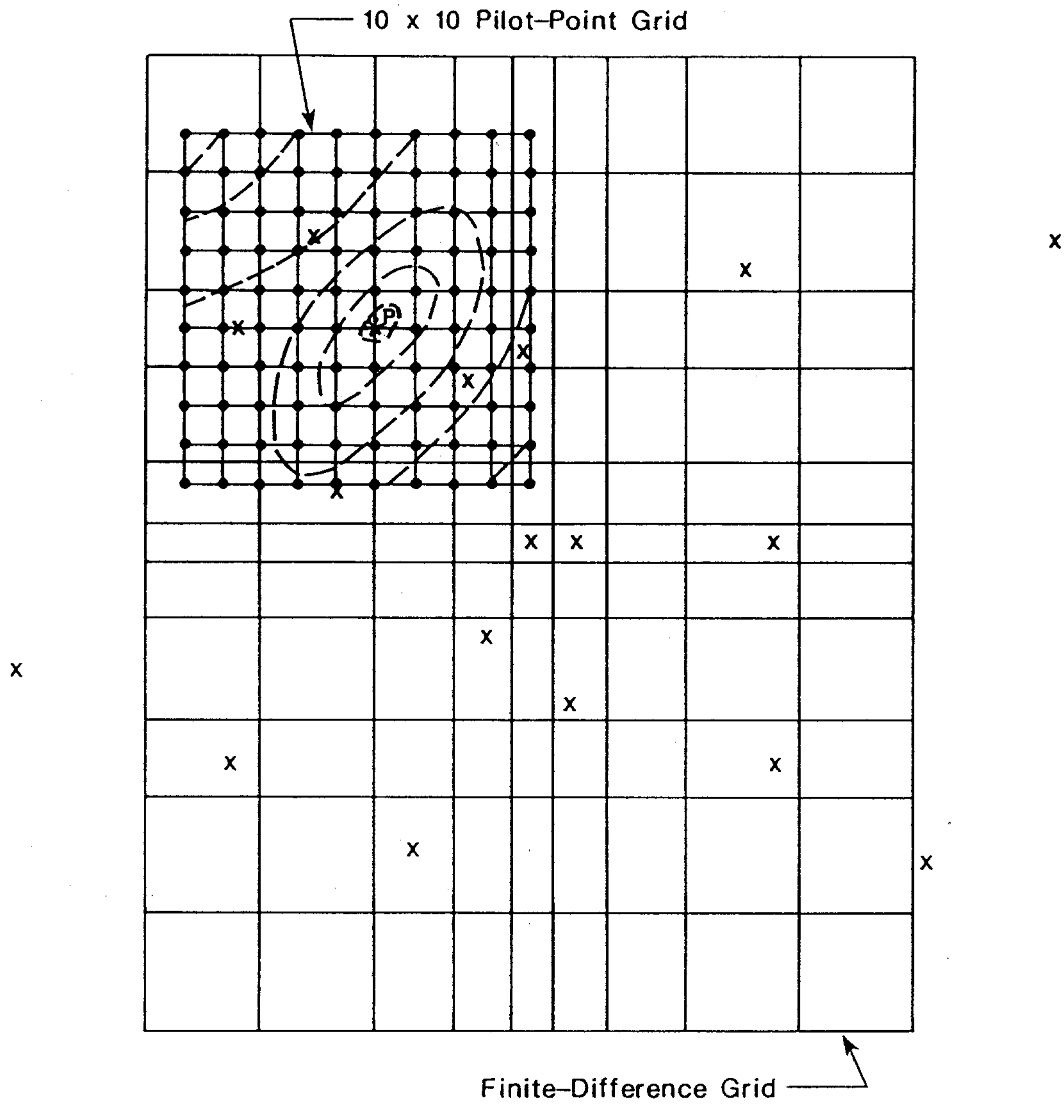

x = Transmissivity Measurement at a Well

• = Candidate Pilot Point

* = Selected Pilot Point

--- Contours of Sensitivities

Drawn by	Date
Checked by	Date
Revisions	Date

Example of a Pilot-Point Grid Superimposed on a Finite-Difference Grid for a Ground-Water Flow Model

INTERA Technologies

Figure 1

are evaluated. Figure 1 also shows an example contour plot of the computed sensitivities. The pilot point with the maximum absolute sensitivity (pilot point P in Figure 1) is chosen in the particular iteration .

Thus, to summarize, the calibration procedure adopted here may be described as an indirect approach, with iterative parameter fitting. A structured inverse formulation with a fully automated algorithm has not been chosen in view of the complexity of the site being modeled. The first step consists of deriving the transmissivity distribution in the model by kriging (using generalized kriging in this study) the measured transmissivities and simulating the pressures and computing the least-square model-fit criterion. If this is not less than the convergence criterion, a second iteration is performed. During this step, a pilot-point location is chosen as explained above and the pilot-point transmissivity is assigned by the modeler. The modified transmissivity distribution in the numerical model is derived by kriging the combined pool of the measured transmissivities and the pilot-point transmissivities. In particular, block kriging is adopted to obtain the geometric mean transmissivities over a grid block. At this stage, the correlation structure of the transmissivity field is not recomputed. Then, by simulating the revised pressures and comparing the new least-square objective function with the convergence criterion, the second iteration is completed. Iterations are repeated until satisfactory convergence is achieved. At the end of the iterations, the correlation structure (as indicated by the generalized covariance function for the generalized kriging used in this study, or by a variogram if universal kriging were adopted) of the assigned pilot-point transmissivities is compared with that of the measured transmissivities for a reasonable agreement. The entire exercise may have to be repeated choosing another structure (variogram or generalized covariance function), if the agreement on correlation structure is not judged satisfactory. The final step, may be called, structure validation. This calibration procedure is illustrated schematically in Figure 2.

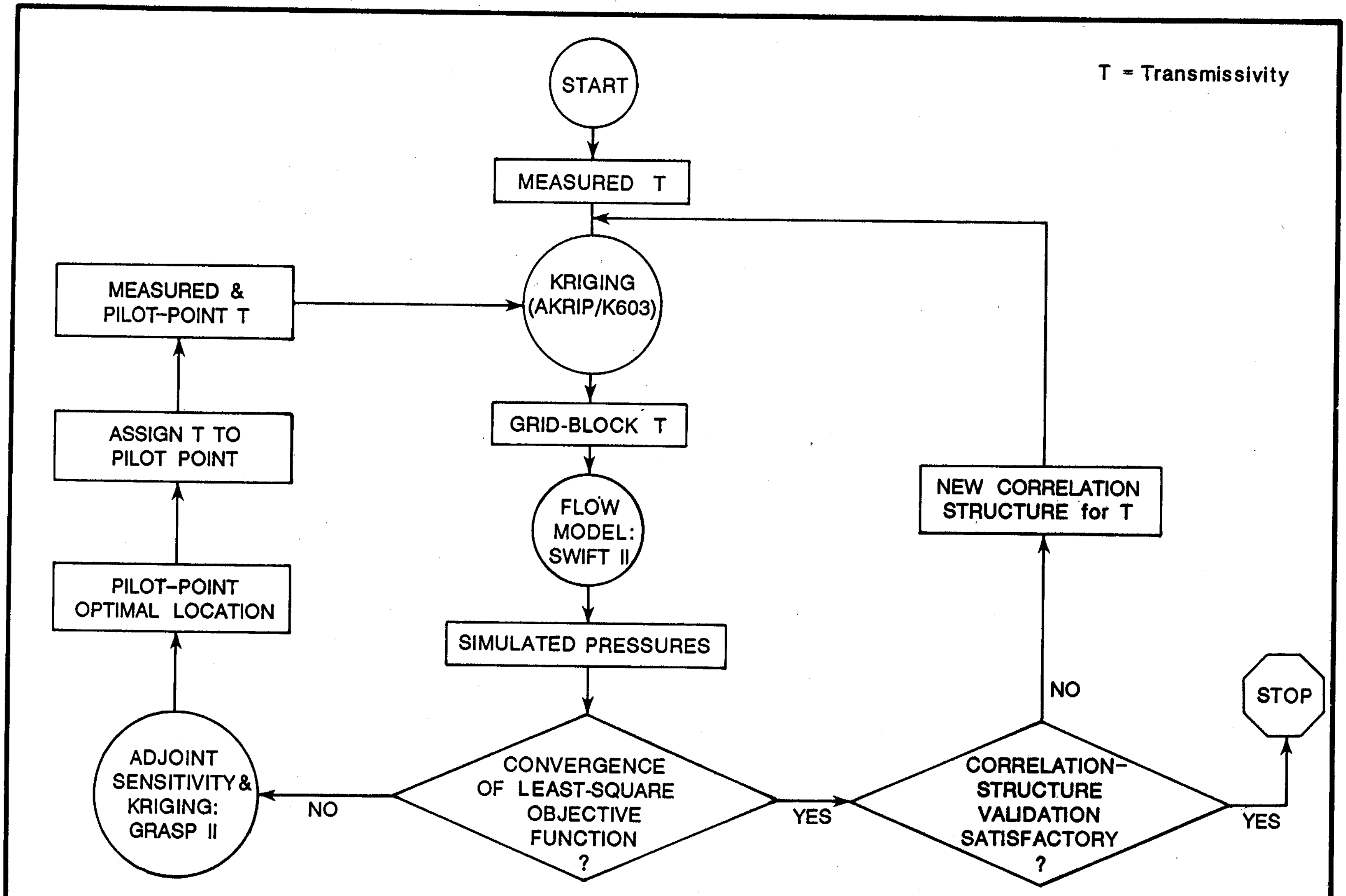

INTERA Technologies | Calibration by Iterative Parameter Fitting: Schematic | Figure 2

This report discusses the development and application of the theory of adjoint-sensitivity analysis to the ground-water flow modeling in the context of model-calibration efforts. An adjoint-sensitivity-analysis code has been built and some of the test problems designed to verify the code performance are also documented in this report. The pilot-point methodology described above has been used with reference to transmissivities only, which are by far, the most important of the parameters. However, the adjoint-sensitivity-analysis code has been built to provide sensitivities with respect to various other parameters, such as storativity, boundary pressures, etc. This document provides the treatment of sensitivity analysis in respect of all the types of hydrogeologic parameters. The remainder of this document is devoted to the mathematical treatment of the adjoint-sensitivity analysis and the verification tests for evaluating the performance of the adjoint-sensitivity code. The report by LaVenue et al (1990) elaborates on the case study involving the application of this calibration approach to the Culebra dolomite at the WIPP site.

SENSITIVITY ANALYSIS: TERMINOLOGY AND SCOPE

Sensitivity analysis of a model provides the first-order derivatives of the functions of output variables with respect to the uncertain input parameters. For the ground-water flow model, the geohydrological parameters, such as the permeability (or transmissivity), storativity, prescribed boundary pressures and fluxes and the strength of point sources or sinks, constitute the sensitivity parameters ($\underline{\alpha}$). Any function of the pressure (or the head) field is designated as the performance measure (J) in the sensitivity-analysis parlance (also called objective function or criterion function). The weighted sum of the squared deviations between the observed and calculated pressures, called the least-square criterion function, where the observations are distributed spatially and temporarily, is an important system performance measure in the model calibration. Darcy velocity, boundary fluxes (where they are not prescribed) and ground-water travel time or distances are all examples of important performance measures. The derivatives, $dJ/d\alpha_i$, are also called marginal-sensitivity coefficients, and provide a first-order estimate of the perturbation ΔJ, in the performance measure J per a unit perturbation ($\Delta\alpha_i=1$) in the sensitivity parameter α_i. Also, the pressure (or the head) function, which depicts the state of the ground-water system is designated as the state function, and the sensitivity of the pressure function as the state sensitivity.

Dimensionless or normalized sensitivity coefficients are defined by $(dJ/d\alpha_i)(\alpha_i/J) = d(\ln J)/d(\ln\alpha_i)$. They denote the percentage perturbation to the performance measure per a 1 percent change in the sensitivity parameter. Caution is necessary in interpreting the normalized sensitivity coefficients, as they may be uninformative and misleading in some situations. For example, when $J = 0$, they assume infinite values; and when $\alpha_i = 0$, they assume zero values and in such situations, marginal sensitivity coefficients are to be used. Also, sensitivity coefficients are exact derivatives taken about the assumed parameter values and therefore constitute local derivatives. They can provide the changes in performance measure due to a 'small' change in sensitivity parameter. However, when large perturbations to sensitivity parameters are considered, they may not be able to provide accurate estimates of the changes in performance measures, if the relationship between the performance measure and the sensitivity parameter is sufficiently non-linear in the neighborhood of the sensitivity parameters.

Sensitivity analysis plays a significant role in ground-water modeling. The sensitivity coefficients provide a deeper insight into the ground-water flow system and aid the modeler in the calibration. They can identify the locations for additional measurements. They are also used to guide a gradient search in the optimization phase of automatic inverse algorithms in ground-water models, for calculation of posterior covariance of the parameters estimated in the inverse algorithm, and for the calculation of the covariance of the predicted pressures (or heads) due to the uncertainty in the parameters (Neuman, 1980a,b; Townley and Wilson, 1985).

An example of the application of the adjoint-sensitivity-analysis technique to ground-water flow systems was by Sykes and Wilson (1984) who performed the parameter sensitivity analysis for a steady-state flow model of the Culebra-dolomite in the Rustler Formation at the WIPP site. They focused attention on the sensitivity of the potentiometric head, with respect to hydraulic conductivities, boundary pressures, and recharge rates. Sykes et al. (1985) performed a similar study on the steady-state flow in the Leadville Formation of the Paradox Basin in Utah, which was then being considered as a potential site for a nuclear-waste repository, extending their analysis further to Darcy velocities as the performance measure, using the same parameters as above. Similar studies (INTERA, 1984a,b,c; Metcalfe et al., 1985) were performed on the parameter-sensitivity analyses of steady-state ground-water flow models in respect to the salt sites in the Paradox and Permian basins and at the Richton dome which were earlier considered as potential sites for a nuclear-waste repository by the U.S. Department of Energy.

GROUND-WATER FLOW MODEL EQUATIONS

In this study, SWIFT II (Sandia Waste Isolation Flow and Transport), a multi-dimensional (up to three dimensions) finite-difference code is used to simulate the ground-water flow. The code can simulate the coupled processes of transport of the fluid, heat, and an inert component (brine) and trace components (radionuclides) in porous or fractured media. The first three processes are treated as coupled through fluid density and viscosity. The code uses the fluid pressure (rather than the head) as the state variable and permeability (rather than the hydraulic conductivity) as the geologic parameter and conservation of mass (rather than volume) to account for the spatially and temporarily variable density and viscosity. The sensitivity-analysis capability is developed at present only for the flow component of the coupled processes. Reeves et al. (1986a,b) document exhaustively the theory and implementation of the SWIFT II code. This code has been extensively verified (Finley and Reeves, 1981; Ward et al., 1984; Reeves et al., 1986c). The governing fluid-flow equations for transient and steady flow are presented here.

<u>Transient-State Flow</u>

$$- \frac{\partial(\phi\rho)}{\partial t} - \nabla \cdot (\rho \underline{u}) + q = 0 \qquad \text{on } R \times [0,\tau] \tag{1}$$

where,

$$\underline{u} = - \frac{\underline{\underline{k}}}{\mu} \cdot (\nabla p - \rho g \nabla z) \tag{2}$$

subject to:

$$p(\underline{x},0) = p_o(\underline{x}) \qquad \text{on } R \tag{3}$$

$$\underline{u} \cdot \underline{n} = \beta(p - P) - Q \qquad \text{on } \Gamma \times [0,\tau] \tag{4}$$

$$\frac{\partial(\phi\rho)}{\partial t} = \frac{\partial(\phi\rho)}{\partial p} \cdot \frac{\partial p}{\partial t} = S \frac{\partial p}{\partial t} \tag{5}$$

Fluid density and porosity are functions of pressure. However, ignoring the second-order effects, the storage coefficient in (5) may be defined approximately as:

$$S(\underline{x}) = \phi_o(\underline{x}) \, \rho_o(\underline{x}) [C_w + C_r(\underline{x})] \tag{6}$$

Here, $\underline{x}$ is vector of spatial coordinates; t is time; $\underline{\underline{k}}$ is permeability tensor (the principal directions of permeability are assumed to coincide with the spatial coordinate directions, resulting in a diagonal matrix for permeability); $p(\underline{x},t)$ is pressure; $\underline{u}(\underline{x},t)$ is Darcy flux vector; $q(\underline{x},t)$ is strength of a source rate; g is acceleration due to gravity; z is the vertical coordinate (positive downward); $\phi_o(\underline{x})$ is initial porosity of rock; $\rho_o(\underline{x})$ is initial density of water; $\phi(\underline{x},t)$ is rock porosity; $\rho(\underline{x},t)$ is density of water; $Q(\underline{x},t)$ is prescribed volumetric influx normal to boundary Γ; $p_o(\underline{x})$ = initial pressure at t = 0; $P(\underline{x},t)$ is prescribed boundary pressure; β dictates the type of boundary condition with $\beta = 0$ indicating Neuman conditions and $\beta \rightarrow \infty$ indicating Dirichlet conditions; $S(\underline{x})$ is aquifer storage coefficient; C_w is compressibility of water; $C_r(\underline{x})$ is compressibility of rock; R is region of interest; Γ is boundary of R; $\underline{n}$ is unit (outward) vector normal to Γ; and $[0,\tau]$ is time interval of interest.

Equation (3) represents the initial conditions. The boundary conditions in (4) have been generalized after Neuman (1980b) and Carrera and Neuman (1986b). Further, SWIFT II can model the effects of a flow system external to the boundary Γ after Carter and Tracy (1960).

Steady-State Flow

$$-\nabla\cdot(\rho_o\underline{u}_o) + q_o = 0 \tag{7}$$

$$\underline{u}_o = -\frac{\underline{\underline{k}}}{\mu}\cdot(\nabla p_o - \rho_o g\nabla z) \qquad \text{on } R \tag{8}$$

$$\underline{u}_o\cdot\underline{n} = \beta\,(p_o - P_o) - Q_o \qquad \text{on } \Gamma \tag{9}$$

Here, $\underline{u}_o$, q_o, p_o, P_o, and Q_o denote the steady-state counterparts of $\underline{u}$, q, p, P, and Q respectively of the transient state.

In SWIFT II, transient analysis always starts at $t = 0$. In some cases, steady-state analysis is performed first, which provides the initial conditions for the transient analysis to be performed in sequence. This is termed sequential steady-and-transient analysis, where the steady-state flow equations may be treated as constraints on the initial conditions.

The ground-water flow problem simulated by SWIFT II, prior to sensitivity analysis, is designated as the 'forward problem', or the 'primary problem'. The sensitivity coefficients, being local derivatives, depend on the hydrogeological parameters used in the forward problem, as well as on the pressure function evaluated in the forward problem.

SENSITIVITY ANALYSIS: DIRECT APPROACH

The performance measure can be defined as:

$$J = \int_0^{\tau} \int_R K(\underline{\alpha}, p(\underline{\alpha}))\, d\underline{x}\, dt \tag{10}$$

Here J = performance measure, K = an appropriately defined kernel function; $p(\underline{\alpha})$ = pressure, and $\underline{\alpha}$ = vector of sensitivity parameters.

If α_1 is the parameter for which sensitivity coefficient is sought,

$$\frac{dJ}{d\alpha_1} = \int_0^{\tau} \int_R \left[\frac{\partial K}{\partial \alpha_1} + \frac{\partial K}{\partial p} \cdot \frac{\partial p}{\partial \alpha_1} \right] d\underline{x}\, dt \tag{11}$$

In (11) J and K need only be Gateaux differentiable (Vainberg, 1964; Saaty, 1967) in order to apply direct sensitivity analysis using (11) (or to apply adjoint methods (Cacuci, 1981)). The first term in the integral on the right-hand side (RHS) of (11) represents the sensitivity resulting from the explicit dependence of J on α_1, and is called the direct effect. The second term in the integral represents an indirect effect due to the implicit dependence of J on α_1 through $p(\underline{\alpha})$. While the computation of the direct effect is a trivial step, that of the indirect effect involves the evaluation of the state sensitivities: $\partial p(\underline{x},t)/\partial \alpha_1$. They may be calculated by the 'parameter-perturbation approach' (Becker and Yeh, 1972; Yeh, 1986) or by solution of the partial-differential equation for state sensitivity (Sykes et al., 1985; Yeh, 1986). But the state sensitivities are required to be recomputed whenever a new parameter is considered. In a numerical model with a large number of grid blocks/elements and different system parameters, this represents an enormous computational effort, being of the same order as in the multiple simulation approach to parameter sensitivity.

An elegant approach suggested by Chavent (1971, 1975) circumvents the need to compute the state sensitivities and thus brings about economy in the computation of sensitivity coefficients. It is called the adjoint-sensitivity approach and is presented here.

SENSITIVITY ANALYSIS: ADJOINT APPROACH

Two alternative procedures are available for the derivation of the adjoint-state equations for a numerical model. The first one is to derive the partial-differential equations for the adjoint-state function starting from those of the ground-water flow, and then to discretize them in the numerical model (Carter et al., 1974; Neuman, 1980b; Sykes et al., 1985; Carrera and Neuman, 1986b). The second procedure is to derive the adjoint state equations for the numerical model directly from the discretized (matrix) equations of ground-water flow (INTERA, 1983b; Sykes and Wilson, 1984; Sykes et al., 1985; Townley and Wilson, 1985). Sykes et al. (1985) intuitively believe the second procedure to prove superior to the first one for the numerical simulation of the adjoint-state function. Townley and Wilson (1985) recognize that the second procedure permits a simpler mathematical treatment, particularly in handling the boundary conditions. Samper and Neuman (1986) have shown that with respect to the advective-dispersive transport equations, both the above formulations are consistent in that they converge to the same adjoint-state partial-differential equations as the spatial and temporal discretization intervals tend to zero. The first procedure has been chosen here. Dogru and Seinfield (1981) used a hybrid procedure by discretizing the equations in the spatial coordinate and deriving the ordinary-differential equation in temporal coordinates.

The following presentation treats the transient-flow case only. Extensions to the steady-state case and the sequential steady-and-transient case readily follow from the treatment given here. The presentation aims to highlight the essential principles of the adjoint theory. The treatment here is patterned after Neuman (1980b) and Carrera and Neuman (1986b), in adopting the first procedure. The treatment of Neuman, and Carrera and Neuman is such that it can provide the sensitivity coefficients only for those parameters included in the analysis initially. The treatment given here is designed to remove such restriction and is generalized to provide the sensitivity coefficients for any arbitrary parameter. This has been achieved by using partial variations (instead of total variations), and keeping the partial variations due to pressure and the parameters distinct. As a result, the sensitivity coefficients for the initial pressures as parameters has been derived here and is not available from any earlier presentation by any author(s). The results for any parameter can be derived from the general formula given here. Further, the use of partial variations brings out vividly the physical significance of the different mathematical steps in the derivation of the equations for the adjoint-state function and the sensitivity coefficients. The treatment here has provided more physical insight into some aspects such as the significance of the adjoint- state function, the choice of the 'final' condition of the adjoint-state function and the link between the steady and transient states in combined analysis of those states.

The performance measure (J), may be defined in general terms as:

$$J = \int_{o}^{\tau} \int_{R} K(\underline{\alpha}, p)\, d\underline{x}\, dt \tag{12}$$

where K is an appropriately defined kernel function.

As an example, K is defined for pressure at location $\underline{x}_1$ and at time t_1, by

$$K(\underline{\alpha}, p) = p(\underline{x}, t)\, \delta(\underline{x} - \underline{x}_1,\ t - t_1) \tag{13}$$

and, for the weighted least-square-error functions, by

$$K(\underline{\alpha}, p) = \sum_{i} \sum_{n} W_{i,n} [p(\underline{x}, t) - p_{ob}(\underline{x}, t)]^2\, \delta(\underline{x} - \underline{x}_i, t - t_n) \tag{14}$$

Here, p_{ob} is an observed pressure. Various other performance measures can be similarly formulated. The dependence of $K(\underline{\alpha}, p)$ on $\underline{x}$ and t is not explicitly displayed.

The first total variation δJ of J is given by (dropping the arguments of K)

$$\delta J = \int_{o}^{\tau} \int_{R} \left(\sum_{i} \frac{\partial K}{\partial \alpha_i} \delta \alpha_i + \frac{\partial K}{\partial p} \delta p \right) d\underline{x}\, dt \tag{15}$$

Defining $\delta_p J$ as the partial variation (Becker, 1964) with respect to pressure and similarly $\delta_{\alpha_i} J$ as the partial variation with respect to parameter α_i,

$$\delta J = \delta_p J + \sum_i \delta_{\alpha_i} J \tag{16}$$

where,

$$\delta_p J = \int_o^{\tau} \int_R \frac{\partial K}{\partial p} \delta p \, d\underline{x} \, dt \tag{17}$$

and

$$\delta_{\alpha_i} J = \int_o^{\tau} \int_R \frac{\partial K}{\partial \alpha_i} \delta \alpha_i \, d\underline{x} \, dt \tag{18}$$

Defining the left-hand side (LHS) of (1) as $\Psi(\underline{\alpha},p)$ and using (5),

$$\Psi(\underline{\alpha},p) = -S \frac{\partial p}{\partial t} - \nabla \cdot (\rho \underline{u}) + q = 0 \qquad \text{on } R \times [o,\tau] \tag{19}$$

Defining the product of the (LHS - RHS) of (4) and the fluid density ρ as $\Psi^*(\underline{\alpha},p)$:

$$\Psi^*(\underline{\alpha},p) = \rho[\underline{u} \cdot \underline{n} - \beta(p-P) + Q] = 0 \text{ on } \Gamma \times [o,\tau] \tag{20}$$

Taking the first total variations of Ψ and Ψ^* and multiplying them by an as-yet-arbitrary but differentiable function $\lambda(\underline{x},t)$ (in anticipation of a computational advantage) and integrating them over $R \times [o,\tau]$ and $\Gamma \times [o,\tau]$ respectively, and defining their sum as $\delta\Omega$,

$$\delta\Omega = \int_o^{\tau} [\int_R \lambda(\underline{x},t) \, \delta\Psi(\underline{\alpha},p) \, d\underline{x} + \int_{\Gamma} \lambda(\underline{x},t) \delta\Psi^*(\underline{\alpha},p) d\underline{x}] \, dt = 0 \tag{21}$$

Here, Ψ^* has been included in (21) to facilitate the treatment of boundary conditions as sensitivity parameters. Expressing $\delta\Omega$ as the sum of the partial variations as in (16)

$$\delta\Omega = \delta_p \Omega + \sum_i \delta_{\alpha_i}\Omega = 0 \tag{22}$$

where (dropping the arguments),

$$\delta_p \Omega = \int_o^\tau \left[\int_R \lambda \delta_p \Psi d\underline{x} + \int_\Gamma \lambda \delta_p \Psi^* d\underline{x} \right] dt \tag{23}$$

and

$$\delta_{\alpha_i}\Omega = \int_o^\tau \left[\int_R \lambda \frac{\partial\Psi}{\partial\alpha_i} \delta\alpha_i \, d\underline{x} + \int_\Gamma \lambda \frac{\partial\Psi^*}{\partial\alpha_i} \delta\alpha_i \, d\underline{x} \right] dt \tag{24}$$

Adding (22) and (16), the first total variation δJ is given by:

$$\delta J = (\delta_p J + \delta_p \Omega) + \sum_i (\delta_{\alpha_i} J + \delta_{\alpha_i} \Omega) \tag{25}$$

In (25), the terms in the first bracket relate exclusively to the variation δp, and those in the second bracket relate exclusively to the variation $\delta\alpha_i$. To render δJ independent of δp (thus, to eliminate the state sensitivities from the required parameter sensitivities), one may choose $\lambda(\underline{x},t)$ to satisfy:

$$\delta_p J + \delta_p \Omega = 0 \tag{26}$$

or,

$$\int_o^\tau \left[\int_R (\delta_p K + \lambda \delta_p \Psi) d\underline{x} + \int_\Gamma \lambda \delta_p \Psi^* d\underline{x} \right] dt = 0 \tag{27}$$

When $\lambda(\underline{x},t)$ satisfies (26) or (27):

$$\delta J = \sum_i (\delta_{\alpha_i} J + \delta_{\alpha_i} \Omega) \tag{28}$$

so that the required sensitivities are given by:

$$\frac{dJ}{d\alpha_i} = \int_o^\tau \{ \int_R \frac{\partial K}{\partial \alpha_i} d\underline{x} + \frac{\partial}{\partial \alpha_i} [\int_R \lambda \Psi \, d\underline{x} + \int_\Gamma \lambda \Psi^* \, d\underline{x}] \} \, dt \tag{29}$$

Equations (27) and (29) constitute the cornerstones of the adjoint theory, and are of immense computational significance. They demarcate the evaluation of sensitivities into two distinct stages, after the solution of the primary or the forward problem. Equation (27) represents the first stage where $\lambda(\underline{x},t)$ is solved for. Equation (29) represents the second stage where the sensitivity coefficients are computed using the function $\lambda(\underline{x},t)$. Equation (27) shows that $\lambda(\underline{x},t)$ depends upon the performance measure (J) and on the system parameters ($\underline{\alpha}$) and the pressure function $p(\underline{x},t)$ from the primary or forward problem. Thus it requires no re-computation if a different sensitivity parameter is to be studied under the same performance measure. Of the two stages, computation of $\lambda(\underline{x},t)$ requires the most computational effort, being the same as that required to evaluate the state function $p(\underline{x},t)$. In the second stage, sensitivity coefficients for a number of parameters can be computed with an additional effort insignificant in comparison to that of the first stage. This aspect is the prime highlight of the adjoint theory and stands in contrast with the direct approach.

ADJOINT-STATE FUNCTION: GOVERNING EQUATIONS

Equation (27) may be transformed to provide the partial-differential equation and the associated initial and boundary conditions for $\lambda(\underline{x},t)$. The details are furnished in Appendix A. The final results are presented here.

Transient-State-Only Case

$$S \frac{\partial \lambda}{\partial t} - \nabla \cdot (\rho \underline{u}_\lambda) + \frac{\partial K}{\partial p} = 0 \quad \text{on } R \times [0,\tau] \tag{30}$$

$$\lambda(\underline{x},\tau) = 0 \quad \text{on } R \text{ at } t = \tau \tag{31}$$

$$\underline{u}_\lambda \cdot \underline{n} = \beta \lambda(\underline{x},t) \quad \text{on } \Gamma \times [0,\tau] \tag{32}$$

where $\underline{u}_\lambda$, named as the adjoint flux is given by:

$$\underline{u}_\lambda = - \frac{\underline{\underline{k}}}{\mu} \cdot \nabla \lambda \tag{33}$$

It is interesting to note that the so-called initial condition on λ is prescribed at the final time $t = \tau$, and not at $t = 0$. More appropriately, it may be designated as the backwards-in-time-initial or final condition. The solution starts at $t = \tau$, proceeds backwards in time, and ends at $t = 0$.

Steady-State-Only Case

The adjoint-state function applicable to the steady state is indicated by $\lambda_o(\underline{x})$. This is distinctly different from $\lambda(\underline{x},0)$, the adjoint-state function relating to the transient state at time $t = 0$. (In fact $\lambda_o(\underline{x})$ is not equal to $\lambda(\underline{x},0)$, even in a sequential steady-and-transient-state analysis and their dimensions are not the same). The equations for this case are derived by defining $\delta\Omega_o$ for steady state analogously to $\delta\Omega$ in (21) and by a parallel treatment from (21) through (27) and through Appendix A.

Solution of $\lambda_o(\underline{x})$:

$$- \nabla \cdot (\rho_o \underline{u}_{\lambda o}) + \frac{\partial K_o}{\partial p_o} = 0 \qquad \text{on } R \tag{34}$$

$$\underline{u}_{\lambda o} \cdot \underline{n} = \beta \lambda_o(\underline{x}) \qquad \text{on } \Gamma \tag{35}$$

where, $\underline{u}_{\lambda o}$, named as steady-state adjoint flux is given by:

$$\underline{u}_{\lambda o} = - \frac{\underline{k}}{\mu} \cdot \nabla \lambda_o \tag{36}$$

and K_o is defined in (37) analogously to K in (12).

$$J_o = \int_R K_o(\underline{\alpha}, p_o) \, d\underline{x} \tag{37}$$

Here, J_o denotes a steady-state performance measure.

Sequential Steady-and-Transient State Case

This is a special case, where the steady-state solution for pressure, provides the initial condition on pressure for further transient simulation. This causes the initial pressures for the transient state solution to be parameter-dependent as opposed to their being regarded as user-prescribed parameters. The equations for this case can be derived by adding $\delta\Omega_o$ for steady state to $\delta\Omega$ in (21) and following the treatment from (21) through (27) and through Appendix A. In this case, (30) through (33) are still applicable for the transient state, while the steady-state solution requires a slight modification of (34) as shown below:

Solution of $\lambda_o(\underline{x})$:

$$- \nabla \cdot (\rho_o \underline{u} \lambda_o) + \frac{\partial K_o}{\partial p_o} + S\lambda(\underline{x},0) = 0 \quad \text{on } R \tag{38}$$

Equations (35) through (37) still apply for the steady-state part of this analysis.

The presence of a storage coefficient, which is a parameter pertinent to the transient state only, in the equation for $\lambda_o(\underline{x})$ appears incongruous at first sight. $\lambda_o(\underline{x})$ denotes ($= dJ/dq_o$, as shown later) the sensitivity of a performance measure defined in the transient state to q_o, a parameter in the steady state. A perturbation of q_o alters the $p_o(\underline{x})$ which consequently changes the performance measure J, so that $\lambda_o(\underline{x}) = dJ/dq_o(\underline{x}) = \int[dJ/dp_o(\underline{x}^*)].[dp_o(\underline{x}^*)/dq_o(\underline{x})]\, d\underline{x}^*$, where the integration is carried over R. It can be shown that $dJ/dp_o(\underline{x}^*) = S\lambda(\underline{x},0)$ so that, $\lambda_o(\underline{x}) = \int[S\lambda(\underline{x}^*,0)].[dp_o(\underline{x}^*)/dq_o(\underline{x})]\, d\underline{x}^*$, where the integration extends over R. Thus, $\lambda_o(\underline{x})$ does depend upon the storage coefficient. Equation (38) can also be derived from this physical conceptualization of the propagation of the perturbations (not presented here).

General Remarks on Adjoint-State Function

Equations (30) through (38) define the boundary and initial value problem for $\lambda(\underline{x},t)$ and/or $\lambda_o(\underline{x})$. The homogeneous parts of the adjoint-state equation and the flow equation are identical and this aspect is exploited in the computer implementation. The boundary conditions for $\lambda(\underline{x},t)$ or $\lambda_o(\underline{x})$ are very simple. At locations of Dirichlet conditions for pressure, the adjoint-state function should be prescribed as zero. Similarly, at locations of Neumann conditions in the flow problem, a zero adjoint flux is to be prescribed. In a numerical code, no additional effort is needed to implement these boundary conditions.

SENSITIVITY COEFFICIENTS

Once the adjoint-state functions $\lambda(\underline{x},t)$ and/or $\lambda_o(\underline{x})$ are computed, the sensitivity coefficients for parameters α_i may be computed with the appropriate equations. For transient-flow-only cases, (29) applies. For steady-state-flow-only cases, the following equation applies:

$$\frac{dJ_o}{d\alpha_i} = \int_R \frac{\partial K_o}{\partial \alpha_i} d\underline{x} + \frac{\partial}{\partial \alpha_i}\left[\int_R \lambda_o \Psi_o d\underline{x} + \int_\Gamma \lambda_o \Psi_o^* \, d\underline{x} \right] \tag{39}$$

where J_o, K_o, Ψ_o, and Ψ_o^* denote the steady-state counterparts of J, K, Ψ, and Ψ^* of the transient cases, and are defined here:

$$\Psi_o\ (\underline{\alpha},p_o) = -\nabla\cdot(\rho_o\underline{u}_o) + q_o = 0 \qquad \text{on } R \tag{40}$$

$$\Psi_o^*\ (\underline{\alpha},p_o) = \rho_o(\underline{u}_o\cdot\underline{n} - \beta(p_o-P_o) + Q_o) = 0 \qquad \text{on } \Gamma \tag{41}$$

J_o and K_o are defined in (37).

For the sequential steady-and-transient analysis, $dJ/d\alpha_i$ is given by the sum of RHS in (29) and (39). The evaluation of these equations is straightforward. However, sensitivity coefficients with respect to permeability need elaboration, firstly since permeability is a tensor, and secondly since it occurs both in the domain equation (Ψ) and in the boundary equation (Ψ^*). The other parameters, however, appear only in one of these equations. Accordingly, permeability and a few other parameters are considered here.

The evaluation of $\partial K/\partial\alpha_i$ or $\partial K_o/\partial\alpha_i$ is handled as follows. Consider two performance measures for transient state:

$$J_1 = \int_0^{\tau}\int_R p(\underline{x},t)\ \delta(\underline{x}-\underline{x}_1,t-t_1)\ d\underline{x}\ dt \ = p(\underline{x}_1,t_1) \tag{42}$$

$$J_2 = \int_0^{\tau}\int_R w(\underline{x},t)\ [p(\underline{x},t)\ -\ p_{ob}(\underline{x},t)]^2\ d\underline{x}dt \tag{43}$$

For both these performance measures $\partial K/\partial \alpha_i = 0$ [see (13) and (14)]. Consider a performance measure in the steady state. Let the Darcy velocity at location $\underline{x}_m$ in the direction i be the performance measure, and the permeability in the direction i be the sensitivity parameter. Then,

$$J_o = \int_R k_i(\underline{x}_m)\ \frac{\partial}{\partial x_i}(p_o\ -\ \rho_o g \nabla z)\ \delta(\underline{x}\ -\ \underline{x}_m)d\underline{x} \tag{44}$$

and

$$\frac{\partial K_o}{\partial k_i(\underline{x}_m)} = \frac{\partial}{\partial x_i}\ (p_o\ -\ \rho_o g \nabla z)\ \delta(\underline{x}\ -\ \underline{x}_m) \tag{45}$$

J_1 in (42) and J_2 in (43) are examples where $\partial K/\partial \alpha_i = 0$, while J_o in (44) is an example where $\partial K_o/\partial \alpha_i$ is not zero as in (45), when $\alpha_i = k_i(\underline{x}_m)$. The non-zero value of $\partial K_o/\partial k_i$ from (45) will be later used in (50).

Permeability

In the SWIFT II code, the coordinate directions are assumed to coincide with the principal directions of the permeability, so that the permeability matrix is diagonal. The permeabilities in the principal directions are indicated by k_i and let x_i denote the coordinate in the direction i (i=1,2,3). The following results are obtained for the transient-flow-only case and later extended to the sequential steady-and-transient case.

Transient Case:

Let $\alpha_i = k_i$ ($i = 1,2,3$) be defined over a region v, interior to the flow domain R. Assuming $\partial K/\partial\alpha_i = \partial K_o/\partial\alpha_i = 0$, and dropping terms independent of $\underline{\underline{k}}$,

$$\frac{dJ}{dk_i} = \int^{\tau} \frac{\partial}{\partial k_i} \{ \int_R \lambda \nabla\cdot[\frac{\rho\underline{\underline{k}}}{\mu} \cdot(\nabla p - \rho g\nabla z)] d\underline{x} - \int_\Gamma \lambda \frac{\rho\underline{\underline{k}}}{\mu} \cdot(\nabla p - \rho g\nabla z)\cdot\underline{n}\, d\underline{x} \} dt \tag{46}$$

Using Green's first identity for the expression in { } in (46),

$$\frac{dJ}{dk_i} = \int_o^{\tau} \frac{\partial}{\partial k_i} \{ -\int_R \nabla\lambda\cdot[\frac{\rho\underline{\underline{k}}}{\mu} \cdot(\nabla p - \rho g\nabla z)] d\underline{x} \} dt \tag{47}$$

$$\frac{dJ}{dk_i} = - \int_o^{\tau}\int_v \frac{\rho}{\mu} \frac{\partial}{\partial x_i} (p - \rho g z) \frac{\partial\lambda}{\partial x_i} d\underline{x}\, dt \tag{48}$$

Sequential Steady-and-Transient Case:

For this case, the contributions from the steady state need to be added in (48). The corresponding equation can be written down by inspection as:

$$\frac{dJ}{dk_i} = - \int_o^{\tau}\int_v \frac{\rho}{\mu} \frac{\partial}{\partial x_i} (p - \rho g z) \frac{\partial\lambda}{\partial x_i} d\underline{x}\, dt - \int_v \frac{\rho_o}{\mu} \frac{\partial}{\partial x_i} (p_o - \rho_o g z) \frac{\partial\lambda_o}{\partial x_i} d\underline{x} \tag{49}$$

Steady-State-Only Case:

Consider the performance measure J_Q defined in (37) for the region of interest v, for the permeability. Using (39) and (45),

$$\frac{dJ_o}{dk_i} = \int_v [\frac{\partial}{\partial x_i} (p_o - \rho_o gz) . \delta(\underline{x}-\underline{x}_m) - \frac{\rho_o}{\mu} \frac{\partial}{\partial x_i} (p_o - \rho_o gz) \frac{\partial \lambda}{\partial x_i}] \, d\underline{x} \quad (50)$$

Pilot-Point Transmissivity

If sufficient measured transmissivity data are available at a site to define the correlation structure of the transmissivity field, geostatistical techniques, such as kriging, can be used to estimate the transmissivities in the modeled region. The correlation structure of the transmissivity data was found to be much better if the logarithm of the transmissivity was used instead of its natural value (de Marsily, 1984). This stems from the fact that the transmissivities are in general, log-normally distributed. In this study, geostatistics has been employed on the logarithms of the transmissivities to the base ten.

Pilot points are locations where the transmissivities are sought to be estimated in this calibration procedure. GRASP II is designed to calculate the sensitivity of any performance measure to the addition of a pilot point (transmissivity) to the observed transmissivity data set used as input for kriging. A number of potential pilot-point locations are considered and the sensitivities of those pilot points are evaluated. The pilot point with the absolute maximum sensitivity is chosen to be included in the transmissivity data during that iteration.

Currently, GRASP II can be used either with the universal kriging code of the United States Geological Survey, K603 (Skrivan and Karlinger, 1980), or with the generalized kriging code of the Massachusetts Institute of

Technology, AKRIP (Kafritsas and Bras, 1981). In addition, either point or block kriging may be specified and uncertainties may be assigned to both observed and pilot-point transmissivity data. The following discussion presents the general equations used to couple the kriging and adjoint-sensitivity techniques.

Let P be a pilot point added to the observation points at a location $\underline{x}_p$ with an assigned transmissivity of T_p. Let $T(\underline{x}_i)$ be the measured transmissivity at location $\underline{x}_i$ and $Y(\underline{x}_i) = \mathrm{Log}_{10}[T(\underline{x}_i)]$. Using the observation points and the pilot point, the kriged (point or block-averaged) value (Y^*) of Y, is given by:

$$Y^*(\underline{x}) = \sum_{i=1}^{n} Y(\underline{x}_i)\ \eta(\underline{x},\underline{x}_i) + Y_p(\underline{x}_p)\ \eta(\underline{x},\underline{x}_p) \tag{51}$$

where

$$Y^*(\underline{x}) = \mathrm{Log}_{10}\ [T^*(\underline{x})] \tag{52}$$

Here, n is the number of observation points, $\eta(\underline{x},\underline{x}_i)$ is the (point or block-averaged) kriging weight for location $\underline{x}$ due to an observation at location $\underline{x}_i$, $Y_p = \mathrm{Log}_{10}[T_p(\underline{x}_p)]$, and T^* is the estimated transmissivity. Note that the following equations are valid for either point or block kriging. The kriging weights would depend upon whether point or block kriging is adopted.

Using (51),

$$\frac{\partial Y^*(\underline{x})}{\partial Y_p(\underline{x}_p)} = \eta(\underline{x},\underline{x}_p) \tag{53}$$

When a pilot point transmissivity is perturbed, the kriged transmissivities and hence the permeabilities at all locations in the flow domain are altered, causing the performance measure to change. Accordingly, the required sensitivity $dJ/dY_p(\underline{x}_p)$ is given by:

$$\frac{dJ}{dY_p(\underline{x}_p)} = \int_R \frac{\partial J}{\partial Y^*(\underline{x})} \frac{\partial Y^*(\underline{x})}{\partial Y_p(\underline{x}_p)} d\underline{x} \tag{54}$$

$$= \int_R \frac{\partial J}{\partial Y^*(\underline{x})} \eta(\underline{x}, \underline{x}p) \; d\underline{x} \tag{55}$$

Also,

$$T^*(\underline{x}) = k^*(\underline{x})[\rho(\underline{x})/\mu(\underline{x})] \; g \; b(x) \tag{56}$$

where b = thickness of ground-water system, and using (52),

$$\frac{dJ}{dY^*(x)} = 2.303 \; \frac{dJ}{dk(\underline{x})} \; k(\underline{x}) \tag{57}$$

so that (55) is rewritten as:

$$\frac{dJ}{dY_p(\underline{x}_p)} = 2.303 \int_R k(\underline{x}) \frac{dJ}{dk(\underline{x})} \eta(\underline{x}, \underline{x}p) d\underline{x} \tag{58}$$

The kriging weights, $\eta(\underline{x},\underline{x}_p)$, determined by GRASP II, are obtained from either the universal kriging code, K603, or from the generalized kriging code, AKRIP. The sensitivity coefficient $dJ/dk(\underline{x})$ in (58) is obtained from adjoint-sensitivity analysis, using equations such as (48), or (49), or (50) depending upon the type of SWIFT II simulation performed.

Boundary Pressure

For simplicity, only the transient state is presented. The boundary pressure P occurs only in the boundary integral of (29), using which,

$$\frac{dJ}{dP} = \int_{o}^{\tau}\int_{\Gamma} \rho\beta\lambda \; d\underline{x}dt \tag{59}$$

However, dJ/dP becomes indeterminate (for Dirichlet boundary conditions) as $\lambda \to o$ and $\beta \to \infty$ at the boundary. Using (32), the RHS of (59) may be rewritten as:

$$\frac{dJ}{dP} = -\int_{o}^{\tau}\int_{\Gamma} \frac{\rho\underline{\underline{k}}}{\mu}\cdot\nabla\lambda\cdot\underline{n} \; d\underline{x}dt \tag{60}$$

<u>Storage Coefficient</u>

Using (29),

$$\frac{dJ}{dS} = -\int_{o}^{\tau}\int_{v} \lambda \frac{\partial p}{\partial t} \; d\underline{x}dt \tag{61}$$

where v denotes the region of interest for the storage coefficient.

Storativity:

Storativity S^* (dimensionless) is more commonly used in ground-water hydrology for vertically integrated two-dimensional flows and is related to the storage coefficient S by:

$$S^* = (S)bg = \phi(C_w + C_r)\rho bg \tag{62}$$

Then (62) is modified:

$$\frac{dJ}{dS^*} = -\int_{o}^{\tau}\int_{v} \lambda \frac{\partial p}{\partial t}\frac{1}{bg} \; d\underline{x}dt \tag{63}$$

Similarly the following sensitivity coefficients are derived using (29) and treating transient state only.

Source Rate

$$\frac{dJ}{dq} = \int_0^\tau \int_V \lambda \, d\underline{x} dt \tag{64}$$

Boundary Flux

$$\frac{dJ}{dQ} = \int_0^\tau \int_\Gamma \rho\lambda \, d\underline{x} dt \tag{65}$$

Initial Pressure

Initial pressures appear in Ψ in (19) only during the first time step, from 0 to Δt, for which $S\delta p/\delta t$ may be expressed as $S[p(\underline{x},\Delta t) - p_o(\underline{x})]/\Delta t$. Then using (29),

$$\frac{dJ}{dp_o(\underline{x})} = S\lambda(\underline{x},0) \tag{66}$$

In view of (66) the term $S\lambda(\underline{x},0)$ on the LHS of (38) may be recognized as $dJ/dp_o(\underline{x})$.

ADJOINT-STATE FUNCTION: PHYSICAL SIGNIFICANCE

Transient State

A scrutiny of (64) provides an insight into the physical significance of the adjoint-state function. Using (64), one may write :

$$dJ = \int_0^{\tau}\int_V \lambda(\underline{x},t)\ dq\ d\underline{x}dt \tag{67}$$

Define:

$$q(\underline{x},t) = q^* \ \delta(\underline{x}-\underline{x}_1, t-t_1) \tag{68}$$

so that

$$\frac{dJ}{dq^*} = \int_0^{\tau}\int_V \lambda(\underline{x},t)\ \delta(\underline{x}-\underline{x}_1,t-t_1)\ d\underline{x}dt = \lambda(\underline{x}_1,t_1) \tag{69}$$

In (68), q^* is the strength of an (instantaneous) impulse source introduced in the flow field at $\underline{x}_1$ and at time t_1. In (69), the adjoint-state function $\lambda(\underline{x},t)$ is interpreted as the sensitivity coefficient for the parameter of instantaneous source strength at $(\underline{x},t)$. It represents the rate at which J varies per unit impulse source at $(\underline{x},t)$.

Steady State

By similar arguments, in steady state,

$$\lambda_o(\underline{x}) = \frac{dJ}{dq_o(\underline{x})} \tag{70}$$

Equation (70) shows that the adjoint-state function $\lambda_o(\underline{x})$ is a sensitivity coefficient for the parameter of (steady state) source rate. It represents the rate at which J (or J_o) varies per unit source rate applied in the steady state. It can be shown that for a numerical model of the steady state, the elements of the hydraulic-resistance matrix (inverse of the hydraulic-conductance matrix) constitute the adjoint states for the pressure function.

Note that the dimensions of the adjoint state in the steady and transient state differ. Such functions are well known in several branches of science under different names. For example, in mathematical physics, they are known as Green's functions; in systems engineering as impulse-response functions; in surface-water hydrology as instantaneous unit hydrograph (IUH); and in adjoint-state theory as importance functions (Lewins, 1964). Similar functions also arise in constrained optimization as Lagrangian multipliers, and in econometric models as shadow prices. The recommended usage in ground-water hydrology would be impulse-source response function in transient state, and unit-source-rate-influence function in steady state.

SENSITIVITY-ANALYSIS CODE: GRASP II

GRASP, GRoundwater Adjoint Sensitivity Program (Wilson et al., 1986), was originally built as a satellite post-processor to the SWENT groundwater flow code (INTERA, 1983a). In the present study, the GRASP code was modified to be a post-processor to the SWIFT II code. The original GRASP code was designed for steady-state analysis. The code capabilities have been further enhanced as described below and the resulting code is named GRASP II. Both versions employ finite-difference approximation to all the results presented here. GRASP II can perform the sensitivity analysis of purely steady or transient flow or sequential steady-and-transient flow analysis. It has several options on the performance measure (J) and sensitivity parameters (α_i). They are listed below:

Performance Measures	Sensitivity Parameters
Weighted mean pressure over a region at any time	Principal permeabilities
Weighted sum of squared deviations between observed and calculated pressures	Storativity/storage coefficient
Darcy velocities (x, y, or z directions)	Boundary pressures
Fluxes at Dirichlet boundary	Source rates
Groundwater travel times	Recharge rates
Groundwater travel distances	Logarithms of pilot-point transmissivities

VERIFICATION OF THE GRASP II CODE

An extensive verification of the GRASP II code has been undertaken encompassing all of the options on the performance measure and sensitivity parameters in the code. Three of the test problems and their results from GRASP II along with the results from an alternative approach (analytical or perturbation approach) are given here. A number of verification problems for the steady-state sensitivity analysis capability, are presented in Wilson et al (1986) and all of them have been used for GRASP II. Only one of those verification problems is included here.

Test problem 1 relates to transient radial flow around a well for which the Theis equation (Theis, 1935) applies. Appendix B provides the sensitivity coefficients for this problem obtained by direct differentiation. Such sensitivity coefficients correspond to the parameters of the entire aquifer and hence verify the sums of the sensitivity coefficients in all the grid blocks. Wilson and Metcalfe (1985) performed similar verification tests for steady flow in a one-dimensional Cartesian aquifer. The sensitivities for the parameters of the individual grid blocks cannot be verified by this procedure. Test problem 3 has been designed to overcome this limitation, which is inherent in using the classical analytical solutions of ground-water flow (transient or steady) applicable to homogeneous systems. Test problem 2 relates to an interim finite-difference model of the regional ground-water flow in the heterogeneous aquifer at the WIPP site, for which verification has been done by the parameter-perturbation approach. Test problem 3 is designed to verify the sensitivity coefficients for the parameters in the individual grid blocks of a finite-difference model. Exact mathematical expressions for the required sensitivity coefficients have been derived by constructing analytical analogs of the numerical model for the special case of steady-state flow in a one-dimensional (Cartesian) aquifer (given in Appendix C). The analysis requires consideration of an inhomogeneous aquifer, the results of which can be applied to the parameters of the grid blocks of a homogeneous aquifer. Test problem 3 relates to steady (Cartesian) one-dimensional flow in an aquifer.

Test Problem 1

This problem (Figure 3), relates to the transient radial flow around a well of radius 0.114 m pumping at a constant rate of 3×10^{-3} m^3/s in a homogeneous confined aquifer with hydraulic conductivity of 3.27×10^{-4} m/s, and of a uniform thickness of 3.05 m (Ward et al., 1984). The porosity and compressibility of the aquifer are taken to be 0.20 and 1.67×10^{-7}/Pascal, respectively. The fluid is treated as incompressible. The external radius of the aquifer is taken to be 6096 m. The initial pressure throughout the aquifer is constant at 59770 Pascals. The boundary pressure prescribed at the external radius is the same as the initial pressure. The flow is simulated using SWIFT II with 50 finite-difference

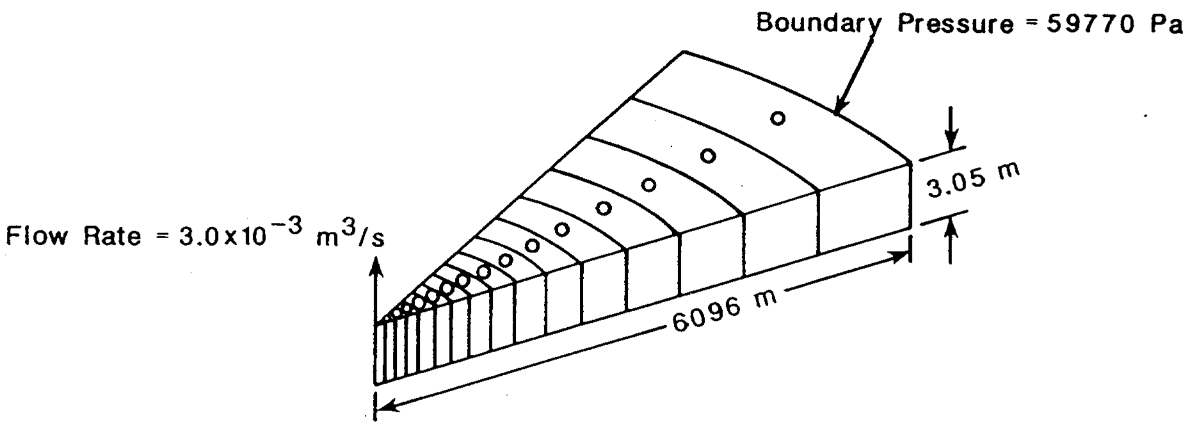

Hydraulic Conductivity = 3.28×10^{-4} m/s

Porosity = 0.20

Rock Compressibility = 1.67×10^{-7}/Pa

Performance Measures:

$J_1 = p(100\ \text{m},\ 3456\ \text{s})$

$J_2 = J_1^{\,2}$

Drawn by	Date	Transient Radial Flow to a Well: Test Problem 1 – Definition Sketch
Checked by	Date	
Revisions	Date	
INTERA Technologies		Figure 3

grid blocks with radial distances to successive grid blocks chosen to be in a geometric sequence. (Such a discretization results in equal pressure drops between successive grid blocks in steady state). Simulations have been performed with uniform time steps in one run, but with different magnitudes of the time steps in different runs. Two performance measures are considered. One is the pressure at radial distance of 100 m from the well at a time of 3456 s. The other is a weighted squared deviation between this calculated pressure and a hypothetical observed pressure at the same spatial and temporal location. For simplicity, the hypothetical observed pressure is taken as zero, and a unit weight is assigned. The second performance measure is simply a square of the first performance measure. The sensitivity parameters considered are the permeability and storativity of the aquifer and the flow rate in the well. Appendix B provides the analytical expressions for the required sensitivity coefficients for this problem.

Table 1 shows the comparison of the GRASP II code results with the analytical results. It is seen that small time steps (40 - 60 s) are required to reproduce the pressure drawdown in the numerical model accurately in comparison with the analytical results (Theis, 1935) for the early times chosen here. For such refined temporal discretization, the GRASP II code results are in exact agreement with the analytical results shown in Appendix B. However, for coarse time steps, SWIFT II results and hence GRASP II results do not agree with the analytical results. But GRASP II results agree well with those from the perturbation approach (not shown here). Thus, if a particular temporal discretization is considered adequate for the numerical modeling of the forward problem (by SWIFT II), the corresponding GRASP II result would be consistent with the level of accuracy in SWIFT II though both SWIFT II and GRASP II may appear to be in error in relation to an analytical solution. Test problem 2 addresses this aspect.

Table 1. Sensitivity Coefficients in Test Problem 1

Perf. Measure	t (sec)	Perf. Measure		Marginal Sensitivity Coefficients					
		SWIFT II Code	Theis Eq.	Permeability		Storativity		Source Rate	
				GRASP II	Analytical	GRASP II	Analytical	GRASP II	Analytical
J_1	57.6	58948.0	58935.3	-8.93×10^{12}	-8.93×10^{12}	1.12×10^{6}	1.13×10^{6}	274.2	278.2
"	86.4	58949.1	58935.3	-8.83×10^{12}	"	1.12×10^{6}	"	273.8	"
"	432.0	58960.9	58935.3	-7.72×10^{12}	"	1.07×10^{6}	"	270.0	"
"	864.0	58971.2	58935.3	-6.46×10^{12}	"	1.02×10^{6}	"	266.4	"
J_2	57.6	3.47×10^{9}	3.47×10^{9}	-1.05×10^{18}	-1.05×10^{18}	1.33×10^{11}	1.34×10^{11}	3.23×10^{7}	3.28×10^{7}
"	86.4	3.47×10^{9}	3.47×10^{9}	-1.04×10^{18}	"	1.32×10^{11}	"	3.23×10^{7}	"
"	432.0	3.48×10^{9}	3.47×10^{9}	-9.10×10^{17}	"	1.26×10^{11}	"	3.18×10^{7}	"
"	864.0	3.48×10^{9}	3.47×10^{9}	-7.62×10^{17}	"	1.20×10^{11}	"	3.14×10^{7}	"

J_1 = Pressure at 100 m, at 3,456 s
$J_2 = J_1^2$

Test Problem 2

This problem relates to a sequential steady-state and transient-state simulation of two-dimensional (x-y) flow in the Culebra dolomite at the Waste Isolation Pilot Plant (WIPP) site. The Culebra is heterogeneous and is discretized by a 26 x 44 finite-difference grid (Figure 4). The transmissivity distribution, boundary conditions and sources/sinks and other details are presented by LaVenue et al. (1988) and are not included here. For purposes of the verification, the simulation is performed up to 10 days only. Time is taken as zero at the end of the steady-state simulation and a hypothetical pumping rate in the well H-3 is adjusted so as to induce large drawdowns in the observation well H-1.

Two performance measures similar to those in test problem 1 are studied. One is the pressure at the location of the H-1 observation well at the end of 10 days. The second performance measure is the weighted squared deviation between the above calculated pressure and a hypothetical observation taken at the same location and at the same time (10 days). For ease of verification, the hypothetical observed pressure is taken to be zero, and the weight as unity. The sensitivity parameters considered are permeability (calculated from transmissivity), storativity, and the time-dependent recharge rate and source rate in the steady state and transient state. Because of the very low permeabilities of the anhydrite and the halite units confining the Culebra, the flow model presented in LaVenue et al. (1988) utilizes an assumption of no recharge or discharge vertically from the Culebra. The recharge rate defined in this test problem is only for the purpose of verification of one of the capabilities of the GRASP II code.

These tests use a perturbation approach for verification. After a base-case simulation using the SWIFT II code, the sensitivity parameter (α_i), such as the recharge rate, is perturbed by a small magnitude ($\Delta\alpha_i$), and the SWIFT II simulation is repeated. The change (ΔJ) in the

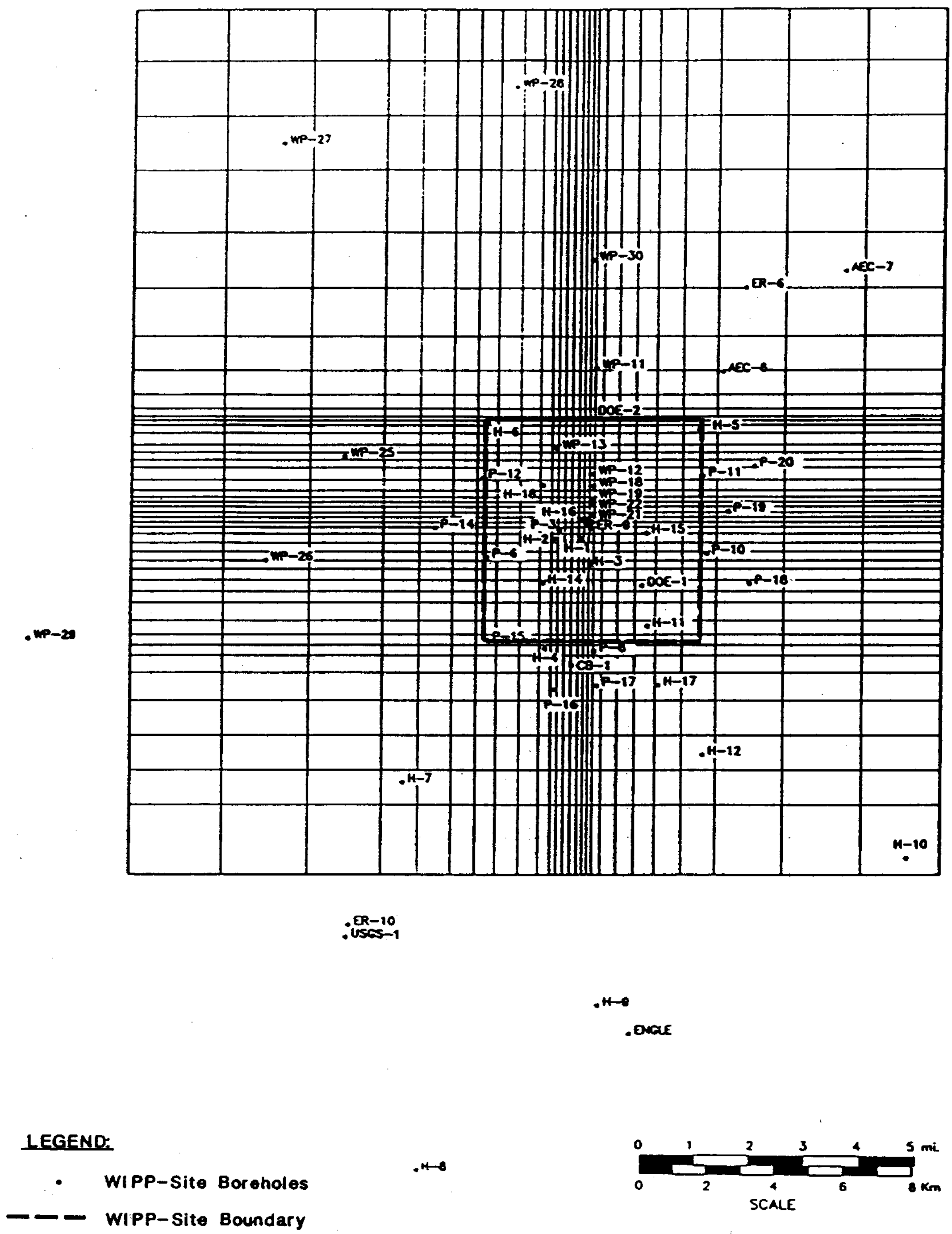

Drawn by	Date
Checked by	Date
Revisions	Date

Steady-and-Transient Flow through a Heterogeneous Two-Dimensional Aquifer: Test Problem 2 - WIPP Model

INTERA Technologies

Figure 4

performance measure (J) between the two simulations is computed. The ratio $\Delta J/\Delta\alpha$ is compared with the sensitivity coefficient computed by the GRASP II code. For some problems, it would be convenient to compute dimensionless sensitivity coefficients. In such a case, $\Delta J/J$ and $\Delta\alpha_i/\alpha_i$ are computed.

In the case of permeability and storativity, SWIFT II simulations have been performed increasing the parameters throughout by one percent and later decreasing them by one percent. For runs where perturbation of the recharge rate is considered, a recharge rate of 10^{-9} m/s is used. One run includes the recharge for steady state only and another run includes it only for transient state. Similar runs for a source rate of 1 kg/s are also performed.

Table 2 presents the sensitivities of both the performance measures to the time-independent parameters (permeability and storativity). Table 3 presents the results for time-dependent parameters of recharge rate and source rate. The agreement between the perturbation approach and the GRASP II code is very good. It is pertinent to note that this good agreement is due to the small perturbations used. For large perturbations, due to the nonlinear relation between the performance measures and the sensitivity parameters, such good agreement would not be obtained. The good agreement secured in this test is also attributable to the fact that the same spatial and temporal discretizations are used in SWIFT II and GRASP II.

Verification of Adjoint States:

Using a finite-difference discretization of (64), adjoint states are given by:

$$\lambda(\underline{x}_1, t_1) = \frac{\Delta J}{\Delta q(\underline{x}_1, t_1)} \frac{1}{\Delta t} \tag{71}$$

Table 2. Sensitivity Coefficients in Test Problem 2: Time-Independent Parameters

Performance Measure	Parameter	Dimensionless Sensitivity Coefficients SWIFT II	Dimensionless Sensitivity Coefficients GRASP II (Perturbation Approach)
p = pressure at H-1 at 10 days	Permeability	4.00	3.99
	Storativity	7.15	7.21
p^2	Permeability	7.93	7.98
	Storativity	-14.30	-14.40

Table 3. Sensitivity Coefficients in Test Problem 2: Time-Dependent Parameters

Performance Measure	Parameter	Marginal Sensitivity Coefficient			
		Steady State Only		Transient State Only	
		SWIFT II	GRASP II	SWIFT II	GRASP II
p=pressure at H-1 at 10 days	Recharge Rate	3.11×10^{16}	3.13×10^{16}	5.85×10^{16}	5.60×10^{16}
	Source Rate	1.23×10^{6}	1.23×10^{6}	1.75×10^{6}	1.70×10^{6}
p^2	Recharge Rate	-2.16×10^{22}	-2.18×10^{22}	-4.07×10^{20}	-3.89×10^{20}
	Source Rate	-8.53×10^{11}	-8.55×10^{11}	-1.22×10^{12}	-1.18×10^{12}

$$\lambda_o(\underline{x}_1) = \frac{\Delta J}{\Delta q_o(\underline{x}_1)} \tag{72}$$

where Δt = time step just prior to t_1 in the numerical model.

Equations (71) and (72) indicate that for one performance measure J, to verify λ in each location $\underline{x}_1$, as many simulations of SWIFT II should be done as the number of such locations, each simulation introducing a source at the location $\underline{x}_1$. Such an enormous computational effort can be saved, in some cases, particularly for the performance measure of pressure by exploiting a "reciprocal relationship" given below:

Reciprocal Relationship:

$$\delta p^{1}_{m}(q^{n}_{k}) = \delta p^{1}_{k}(q^{n}_{m}) \tag{73}$$

Equation (73) states that the pressure rise at location k due to a source at a location m is the same as the pressure rise at location m due to a source at location k, when both the pressure rises are referred to the same time level 1 and the sources are introduced during the same time step n. This is a special case of Maxwell's reciprocal relationships (Michalos and Wilson, 1965; Morse and Feshbach, 1953) valid in several disciplines of continuum mechanics, as adapted to ground water. This result can be deduced from the symmetry of the conductance and storativity matrices in an inhomogeneous aquifer. Equation (73) obviates the need for repeated simulations. One simulation with a source at the location of the grid block, the pressure in which is defined as the performance measure, would suffice for the verification of λ for all locations. The adjoint states for the steady state and transient state are displayed in Table 4 and show good agreement between the results of GRASP II and those of the perturbation approach.

Table 4. Adjoint-State Function in Test Problem 2

Grid Block (I,J)	Adjoint State Function: Steady State — SWIFT II (Perturbation Approach)	Steady State — GRASP II	Transient State — SWIFT II (Perturbation Approach)	Transient State — GRASP II
(14,7)	1.30×10^6	1.30×10^6	0.887	0.861
(15,7)	1.23×10^6	1.23×10^6	2.022	1.960
(15,6)	9.37×10^5	9.37×10^5	0.226	0.218

Test Problem 3

Consider a one-dimensional homogeneous aquifer, discretized into 5 grid blocks each 200 m in length, and subjected to prescribed pressures at both ends. The resulting pressure distribution is linear, and the Darcy velocity is constant throughout the aquifer. The fluid and the aquifer properties are adjusted to result in a hydraulic conductivity of 1.0 m/s. The pressure gradient is adjusted to yield a Darcy velocity of 0.1 m/s. The geometry, geohydrologic and fluid properties, and the prescribed pressures are shown in Figure 5.

Sensitivity coefficients for many combinations of performance measures and model parameters were computed with GRASP II for test problem 3 and they were compared in Table 5 to the sensitivity coefficients computed with the analytical solutions presented in Appendix C. The GRASP II results show exact agreement with the analytical results.

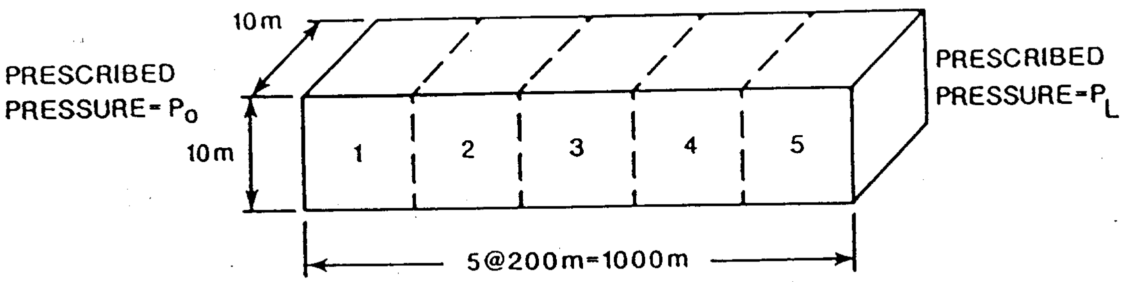

a) Definition Sketch

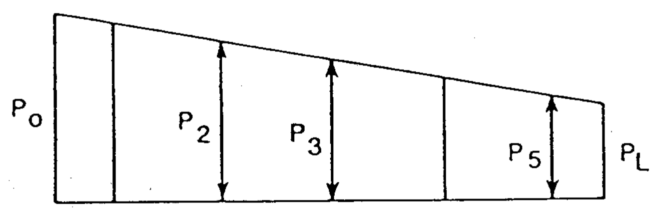

b) Pressure Distribution

Boundary Conditions

$P_o = 1.962 \times 10^6$ Pa

$P_L = 9.810 \times 10^5$ Pa

Geohydrologic Parameters

permeability = $1.02 \times 10^{-7} m^2$

density = 10^3 kg/m^3

viscosity = 10^{-3} Pa-s

(hydraulic conductivity = 1.0 m/s)

Geometry

$\Delta x = 200$m

N = 5

$\Delta y = z = 10$m

Drawn by	Date	Steady Flow through One-Dimensional Homogeneous Aquifer: Test Problem 3 - Definition Sketch
Checked by	Date	
Revisions	Date	
INTERA Technologies		Figure 5

Table 5. Sensitivity Coefficients in Test Problem 3

Performance Measure J	Sensitivity Parameter α	Sensitivity Coefficient, $dJ/d\alpha$ GRASP II	Analytical Solution
P_2	k_1	1.347×10^{12}	1.347×10^{12}
	k_2	3.849×10^{11}	3.849×10^{11}
	k_3	-5.774×10^{11}	-5.774×10^{11}
	P_o	7.000×10^{-1}	7.000×10^{-1}
	P_L	3.000×10^{-1}	3.000×10^{-1}
	Q_3	2.943×10^{7}	2.943×10^{7}
	Q_4	1.766×10^{7}	1.766×10^{7}
	q_1	6.867×10^{0}	6.867×10^{0}
	q_2	2.060×10^{1}	2.060×10^{1}
	q_3	1.471×10^{1}	1.471×10^{1}
J_2	k_1	1.510×10^{17}	1.510×10^{17}
	k_2	-7.553×10^{16}	-7.553×10^{16}
	k_3	-1.510×10^{17}	-1.510×10^{17}
	P_o	1.570×10^{5}	1.570×10^{5}
	P_L	-1.570×10^{5}	-1.570×10^{5}
	Q_2	3.080×10^{12}	3.080×10^{12}
	Q_4	-3.080×10^{12}	-3.080×10^{12}
	q_1	1.540×10^{6}	1.540×10^{6}
	q_2	1.540×10^{6}	1.540×10^{6}
	q_4	-1.540×10^{6}	-1.540×10^{6}

Table 5. Sensitivity Coefficients in Test Problem 3
(Continued)

Performance Measure J	Sensitivity Parameter α	Sensitivity Coefficient, $dJ/d\alpha$ GRASP II	Sensitivity Coefficient, $dJ/d\alpha$ Analytical Solution
u_2	k_1	1.962×10^{5}	1.962×10^{5}
	k_2	1.962×10^{5}	1.962×10^{5}
	P_o	1.020×10^{-7}	1.020×10^{-7}
	P_L	-1.020×10^{-7}	-1.020×10^{-7}
	Q_1	2.000×10^{0}	2.000×10^{0}
	Q_3	-1.000×10^{1}	-1.000×10^{1}
	q_1	1.000×10^{-6}	1.000×10^{-6}
	q_3	-5.000×10^{-6}	-5.000×10^{-6}
F_o	k_1	1.962×10^{10}	1.962×10^{10}
	P_o	1.020×10^{-2}	1.020×10^{-2}
	Q_2	-1.400×10^{6}	-1.400×10^{6}
	q_3	-5.000×10^{-1}	-5.000×10^{-1}
t'†	k_1	-1.962×10^{9}	-1.962×10^{9}
	k_2	-1.962×10^{9}	-1.962×10^{9}
x'‡	k_1	1.962×10^{9}	1.962×10^{9}
	k_2	1.962×10^{9}	1.962×10^{9}

† Time of travel from one end of the system to the other end.

‡ Displacement during time t'.

Table 5. Sensitivity Coefficients in Test Problem 3
(Continued)

LEGEND

Performance Measures

p_i = modeled pressure for grid block i
u_i = modeled centroidal Darcy velocity for grid block i
F_o = boundary flux at x = 0 (upgradient boundary)
t' = travel time between x = 0 and x = 1,000 m
x' = displacement during the time t'

$$J_2 = \sum_{i=1}^{5} w_i (p_i - p_{ob_i})^2$$

where,

w_i = 0.2 for all i
p_{ob_i} = 1.4715×10^6 Pa, for all i (equal to computed pressure p_3)

Parameters

k_i = permeability of grid block i
Q_i = recharge to grid block i
q_i = source rate for grid block i
P_o = prescribed pressure at upgradient boundary
P_L = prescribed pressure at x = L; downgradient boundary

SUMMARY AND CONCLUSIONS

Numerical models of a ground-water flow system need to be calibrated, prior to their application in a predictive role. Many alternative methods for the calibration are available, ranging from purely subjective trial-and-error procedures to fully automated inverse algorithms. In this report, the methodology adopted for the calibration of the numerical model of regional ground-water flow in the Culebra dolomite at the Waste Isolation Pilot Plant site has been described. An indirect approach, based on an iterative parameter-fitting procedure, has been adopted for calibration. Parameterization has been effected by choosing to assign the transmissivities only at a few selected locations, designated as pilot points. The transmissivity distribution in the numerical model is derived by kriging the transmissivities in the combined pool of measurement and pilot points. Sensitivity analysis has been coupled with kriging to determine the optimal location of the pilot points. The associated transmissivity at a pilot point has been assigned by the best judgement of the modeler. This judgement utilizes information on local geologic conditions and lagre-scale hydraulic interference tests. The modeler handles one or a few pilot points in one iteration and brings about a consequential change in the transmissivity distribution in the entire model via kriging. The iterative steps of adding pilot point(s) and kriging have been continued until the desired convergence is achieved in the least-square objective function. At the end of all iterations, it is ensured that the correlation structure of the transmissivities at all the pilot points, is in reasonable agreement with that of the measured transmissivity data.

The adjoint approach to sensitivity analysis provides an efficient algorithm for the computation of the sensitivity derivatives required for the optimal location of pilot points, in contrast to a direct approach. The adjoint strategy consists in separating the sensitivity analysis into two distinct stages, with the first one relating exclusively to the criterion function and the second one relating exclusively to the sensitivity parameters. The adjoint-state function computed in the first stage provides the link between the two stages. Implementing this philosophy, the equations of the sensitivities are derived by keeping the treatment of the partial variations with respect to the pressure and the parameters distinct. The adjoint-state function is interpreted to be an impulse-source response function in the transient state (analogous to the instantaneous unit hydrograph in surface-water hydrology), and a unit-source-rate influence function in the steady state.

A three-dimensional finite-difference code for sensitivity analysis, GRASP II, has been built as a satellite to the flow code SWIFT II. GRASP II can be applied in purely transient or steady flow analyses or in a sequential steady-and-transient flow analysis. It can provide the sensitivities of such direct and indirect output functions of the flow code as pressures, fluxes, ground-water travel times and distances, to all the geohydrological parameters, and the imposed hydraulic stresses. An extensive verification of GRASP II, encompassing all of the options provided in the code, has been conducted by comparing the code output with the results from alternative approaches such as analytical results and parameter-perturbation approaches. Differentiation of classical analytical solutions in ground-water flow provides sensitivities for the parameters of the entire ground-water system. Such sensitivities verify the sums of the sensitivities in all the grid blocks of a numerical model. This approach has been used both for transient and steady flow cases. The limitation inherent in this approach, that the verification relates only to the sums of the sensitivity coefficients, has been removed for the special case of the steady-state flow in a one-dimensional (Cartesian) aquifer by constructing the analytical analog of the numerical model and deriving the exact mathematical expressions for the sensitivity coefficients for the individual grid blocks in the model for verification. An efficient verification scheme has also been made possible by exploiting Maxwell's reciprocal relationships adapted to ground-water flow.

In this report, the theory of the adjoint-sensitivity analysis, as applied to the ground-water flow model has been described, together with three verification test problems. The application of the coupled kriging-and-adjoint-sensitivity approach using pilot points to the calibration of a ground-water flow model of the Culebra dolomite at the Waste Isolation Pilot Plant site in southeastern New Mexico is presented in LaVenue et al (1990). This application has demonstrated the usefulness of the present approach, particularly while handling a combination of the steady and transient head data.

Notation

b	-	thickness of ground-water system
C_r	-	compressibility of rock
C_w	-	compressibility of water
J	-	performance measure: transient state
J_o	-	performance measure: steady state
k	-	permeability of a homogeneous isotropic aquifer
k_i	-	principal permeability in the coordinate direction i
$\underline{\underline{k}}$	-	permeability tensor
K	-	a function for transient state defined in (12)
K_o	-	a function for steady state defined in (37)
p	-	pressure: transient state
P	-	prescribed boundary pressure: transient state
p_o	-	pressure: steady state
p_{ob}	-	observed pressure
P_o	-	prescribed boundary pressure: steady state
q	-	source rate: transient state
q_o	-	source rate: steady state
q^*	-	strength of an impulse source
Q	-	prescribed volumetric influx normal to Γ: transient state
Q_o	-	prescribed volumetric influx normal to Γ: steady state
R	-	flow domain
S	-	aquifer storage coefficient; (6)
S^*	-	aquifer storativity; (62)
t	-	time
T	-	measured transmissivity
T^*	-	estimated transmissivity
$\underline{u}$	-	Darcy flux vector: transient state
$\underline{u}_\lambda$	-	adjoint flux vector: transient state
$\underline{u}_{\lambda o}$	-	adjoint flux vector: steady state
$\underline{u}_o$	-	Darcy flux vector: steady state
v	-	region of interest for a sensitivity parameter

w - weight for the observed pressure

$\underline{x}$ - vector of spatial coordinates

x_i - element i in $\underline{x}$; (i = 1,2,3)

Y - $\text{Log}_{10}(T)$

Y^* - kriged value of Y

z - vertical coordinate

$\underline{\alpha}$ - vector of sensitivity parameter

α_i - element i of $\underline{\alpha}$

β - a parameter to identify the type of boundary condition

$\beta = 0$ for Neumann conditions

$\beta \to \infty$ for Dirichlet conditions

$\delta(.)$ - Dirac delta function

δJ - total variation of J

δV - change of V over a time step

$\delta_p J$ - partial variation of J with respect to p

∇ - gradient operator

ϕ - rock porosity

ϕ_o - initial rock porosity

Γ - boundary of flow domain

$\eta(\underline{x},\underline{x}_j)$ - kriging weight for location $\underline{x}$, due to an observation at $\underline{x}_j$

λ - adjoint-state function: transient state

λ_o - adjoint-state function: steady state

μ - viscosity of water

Ψ - defined in (19) for the flow domain:transient state

Ψ^* - defined in (20) for the flow boundary: transient state

Ψ^*_o - defined in (41) for the flow boundary: steady state

Ψ_o - defined in (40) for the flow domain: steady state

ρ - density of water

ρ_o - initial density of water

τ - final time of flow analysis

Ω - defined in (21)

REFERENCES

Becker, L., and W.W-G. Yeh, 1972. Identification of parameters in unsteady open-channel flows, Water Resources Research, Vol. 8, No. 4, 956-965.

Becker, M., 1964. The Principles and Applications of Variational Methods. Cambridge, Mass., The M.I.T. Press.

Cacuci, D. G., 1981. Sensitivity theory for nonlinear systems, I, Nonlinear functional analysis approach, J. Math. Phys., 22(12), 2794-2802.

Carrera, J. and S.P. Neuman, 1986a. Estimation of aquifer parameters under transient and steady state conditions, 1, Maximum likelihood method incorporating prior information, Water Resources Research, Vol. 22, No. 2, p. 199-210.

Carrera, J. and S.P. Neuman, 1986b. Estimation of aquifer parameters under transient and steady state conditions, 2, Uniqueness, stability, and solution algorithms, Water Resources Research, Vol. 22, No. 2, p. 211-227.

Carter, R.D., L.F. Kemp, Jr., A.C. Pierce, and D.L. Williams, 1974. Performance matching with constraints, Soc. Pet. Eng. J., 14(2), p. 187-196.

Carter, R.D. and C.W. Tracy, 1960. An Improved Method for Calculating Water Influx, Transactions of the Society of Petroleum Engineers, American Institute of Mining Engineers, 219, 415-417.

Chavent, G., 1971. Analyse fonctionelle et identification de coefficients repartis des les equations aux derivees partielles, these de Docteur es Sciences, University of Paris, VI.

Chavent, G., 1975. History matching by use of optimal control theory, Soc. Pet. Eng. J., 15(1), 74-86.

de Marsily, G., G. Lavendau, M. Boucher, and G. Fasanino, 1984. Interpretation of interference tests in a well field using geostatistical techniques to fit the permeability distribution in a reservoir model, in "Geostatistics for Natural Resources Characterization," edited by G. Verly, M. David, A.G. Journel, and A. Marechal, pp. 831-849, D. Reidel, Hingham, Mass.

de Marsily, G., 1986. Quantitative Hydrogeology, Groundwater Hydrology for Engineers, Academic Press, Inc., New York, 440 p.

Dogru, A.H. and J.H. Seinfeld, 1981. Comparison of sensitivity coefficient calculation methods in automatic history matching, Soc. Pet. Eng. J., 21, 551-557, 1981.

Finley, N.C., and M. Reeves, 1981. SWIFT Self-Teaching Curriculum: Illustrative Problems to Supplement the User's Manual for the Sandia Waste-Isolation Flow and Transport Model (SWIFT), Sandia National Laboratories, NUREG/CR-1968, SAND81-0410, 169 p.

INTERA Environmental Consultants Inc., 1983a. SWENT: A Three Dimensional Finite Difference Code for the Simulation of Fluid, Energy and Solute Radionuclide Transport, ONWI-457, 583 pp, Office of Nuclear Waste Isolation, Battelle Memorial Institute, Columbus, Ohio.

INTERA Environmental Consultants Inc., 1983B. "Adjoint Sensitivity Theory for Steady-State Ground-Water Flow", Prepared for Office of Nuclear Waste Isolation, Battelle Memorial Institute, Columbus, Ohio, BMI/ONWI-515.

INTERA Environmental Consultants Inc., 1984A. First Status Report on Regional and Local Ground-Water Flow Modeling for the Richton Dome, Mississippi. Prepared for Office of Nuclear Waste Isolation, Battelle Memorial Institute, Columbus, Ohio, ONWI-502.

INTERA Environmental Consultants Inc., 1984b. First status report on Regional Ground-Water Flow Modeling for the Paradox Basin, Utah. Prepared for Office of Nuclear Waste Isolation, Battelle Memorial Institute, Columbus, Ohio, ONWI-503.

INTERA Environmental Consultants Inc., 1984c. First Status Report on Regional Ground-Water Flow Modeling for the Paradox Basin, Texas. Prepared for Office of Nuclear Waste Isolation, Battelle Memorial Institute, Columbus, Ohio, ONWI-504.

Kafritsas, J. and R.L. Bras, 1981. The Practice of Kriging, Technical Report 263, Ralph M. Parsons Lab., Massachusetts Institute of Technology, Cambridge, Massachusetts, 107 p.

LaVenue, A.M., A. Haug, and V.A. Kelley, 1988. Numerical Simulation of Groundwater Flow in the Culebra Dolomite at the Waste Isolation Pilot Plant (WIPP) Site: Second Interim Report. Sandia National Laboratories, Contractor Report, SAND88-7002.

LaVenue, A.M., J.F. Pickens, and T.L. Cauffman, 1990. Ground-Water Flow Modeling of the Culebra Dolomite, Volume I, Model Calibration. Sandia National Laboratories, Contractor Report SAND89-7068/1.

Lewins, J., 1964. Importance: The Adjoint Function. Pergamon, New York.

Metcalfe, D.E., J.E. Campbell, B.S. RamaRao, and W.V. Harper, 1985. Geostatistical and Adjoint Sensitivity Techniques Applied to a Conceptual Model of Ground-Water Flow in the Paradox Basin, Utah. Paper presented at Waste Management '85, Univ. of Arizona, Tucson.

Michalos, J. and E.N. Wilson, 1965. Structural Mechanics and Analysis. Macmillan Company, London, p. 155.

Morse, P.M. and Feshbach, J, 1953. Methods of Theoretical Physics. McGraw-Hill Book Co., Inc., New York, p. 858.

Neuman, S.P., 1980a. A Statistical Approach to the Inverse Problem of Aquifer Hydrology, 3, Improved Solution Method and Added Perspective. Water Resources Research, Vol. 16, No. 2, p. 331-346.

Neuman, S.P., 1980b. Adjoint-state Finite Element Equations for Parameter Estimation. Paper presented at 3rd International Conference on Finite Elements in Water Resources, Univ. of Miss., Oxford, May 19-23.

Reeves, M., D.S. Ward, N.D. Johns, and R.M. Cranwell, 1986a. Theory and Implementation for SWIFT II, the Sandia Waste-Isolation Flow and Transport Model, Release 4.84. Sandia National Laboratories, NUREG/CR-3328 and SAND83-1159, 189 p.

Reeves, M., D.S. Ward, N.D. Johns, and R.M. Cranwell, 1986b. Data Input Guide for SWIFT II, The Sandia Waste-Isolation Flow and Transport Model for Fractured Media, Release 4.84. Sandia National Laboratories, NUREG/CR-3162 and SAND83-0242, 144 p.

Reeves, M., D.S. Ward, P.A. Davis, and E.J. Bonano, 1986c. SWIFT II Self-Teaching Curriculum: Illustrative Problems for the Sandia Waste Isolation Flow and Transport Model for Fractured Media, Sandia National Laboratories, NUREG/CR-3925, SAND84-1586, 96 p.

Saaty, T.L., 1967. Modern Nonlinear Equations, McGraw-Hill, New York,.

Samper, F.J. and S.P. Neuman, 1986. Adjoint State Equations for Advective-Dispersive Transport, in Finite Elements. Water Resources, Proc. 6th Int. Conf., Lisbon, Portugal, pp 423-438.

SKI, 1984. International Nuclide Transport Code Intercomparison Study, Final Report Level 1. SKI 84:3, Swedish Nuclear Power Inspectorate.

Skrivan, J. and M. Karlinger, 1980. Semi-Variogram Estimation and Universal Kriging Program, U.S. Geological Survey Technical Report PB81-120560, 98 p., Tacoma, Washington.

Sykes, J.F. and J.L. Wilson, 1984. Adjoint Sensitivity Theory for the Finite Element Method. Paper presented at 5th International Conference on Finite Elements in Water Resources, Burlington, Vermont, U.S.A., June, 1984.

Sykes, J.F., J.L. Wilson, and R.W. Andrews, 1985. Sensitivity Analysis for Steady State Groundwater Flow Using Adjoint Operators. Water Resources Research, Vol. 21, No. 3, p. 359-371.

Theis, C.V., 1935. The Relation Between the Lowering of the Piezometric Surface and the Rate and Duration of Discharge of a Well Using Groundwater Storage. Trans. Am. Geophys. Union, Ann. Meet., 16th, p. 519-524.

Townley, L.R. and J.L. Wilson, 1985. Computationally Efficient Algorithms for Parameter Estimation and Uncertainty Propagation in Numerical Models of Groundwater Flow. Water Resources Research, Vol. 21, No. 1, p. 1851-1860.

Vainberg, M.M., 1964. Variational Methods for the Study of Nonlinear Operators. Holden-Day, San Francisco, Calif.

Ward, D.S., M. Reeves, and L.E. Duda, 1984. Verification and Field Comparison of the Sandia Waste-Isolation Flow and Transport Model (SWIFT). Sandia National Laboratories, NUREG/CR-3316, SAND83-1154.

Wilson, J.L. and D. Metcalfe, 1985. Illustration and Verification of Adjoint Sensitivity Theory for Steady State Groundwater Flow. Water Resources Research, Vol. 21, No. 3, p. 1602-1610.

Wilson, J.L., B.S. RamaRao, and J.A. McNeish, 1986. GRASP: A Computer Code to Perform Post-SWENT Adjoint Sensitivity Analysis of Steady State Groundwater Flow. Prepared for Office of Nuclear Waste Isolation, Battelle Memorial Institute, Columbus, OH, BMI/ONWI-625.

Yeh, W.W-G., 1986. Review of Parameter Identification Procedures in Groundwater Hydrology: Inverse Problem. Water Resources Research, Vol. 22, No. 2, p. 95-108.

APPENDIX A: EQUATIONS OF THE ADJOINT-STATE FUNCTION

Equation (27), reproduced here as (A1), is transformed to provide the partial-differential equation for $\lambda(\underline{x},t)$.

$$\int_0^\tau [\int_R (\delta_p K + \lambda \delta_p \Psi] d\underline{x} + \int_\Gamma \lambda \delta_p \Psi^* d\underline{x}] dt = 0 \tag{A1}$$

where

$$\int_0^\tau \int_R \lambda \delta_p \Psi d\underline{x}\ dt = \int_0^\tau \int_R \{ - S\lambda \frac{\partial(\delta p)}{\partial t} - \lambda \nabla \cdot (\rho \delta_p \underline{u}) \} d\underline{x} dt \tag{A2}$$

$$\delta_p \underline{u} = - \frac{\underline{\underline{k}}}{\mu} \cdot \nabla(\delta p) \tag{A3}$$

$$\int_0^\tau \int_\Gamma \lambda \delta_p \overset{*}{\Psi} d\underline{x}\ dt = \int_0^\tau \int_\Gamma \lambda \rho (\delta_p \underline{u} \cdot \underline{n} - \beta \delta p) d\underline{x} dt \tag{A4}$$

While developing the partial variation $\delta_p \Psi$ in (A2), an additional term due to the variation of density with pressure, given by $\partial/\partial\rho[\nabla \cdot \delta_p \underline{u}].(\partial\rho/\partial p).\delta p$, where $[\partial\rho/\partial p]/\rho_o = C_w$ = compressibility of water, needs to be included. As this term is smaller than the other terms by several orders of magnitude due to the practically negligible compressibility of water, it is ignored. Similar terms in $\delta_p \Psi^*$ are also ignored. Further, note that while developing $\delta_p \Psi$ and $\delta_p \Psi^*$, the partial variations with respect to pressure, partial variations with respect to parameters such as permeability and source rate are, by definition, ignored.

The individual terms in (A1) are developed below. Integrating by parts in time domain,

$$\int_{o}^{\tau}\int_{R} S\lambda \frac{\partial(\delta p)}{\partial t}\, d\underline{x}dt = -\int_{R} \left(-\int_{o}^{\tau}(S \frac{\partial\lambda}{\partial t} \delta p)dt + [S\lambda\delta p]_{o}^{\tau}\right) d\underline{x} \tag{A5}$$

One chooses λ to be zero at $t = \tau$ (and for $t > \tau$); $\lambda(\underline{x},\tau) = 0$. This may be designated as the backwards-in-time-initial, or final condition. Fulfillment of this condition would necessitate the evaluation of λ backwards in time from $t = \tau$ to $t = 0$. The choice of the final condition on λ is dictated by physical considerations. It is evident that the performance measure defined at a particular time, is unaffected by a change in the parameters at a later time. For example, the pressure at a location at 30 days after pumping, does not change if the pumping rate changes after 30 days. Thus, the sensitivity of the pressure at 30 days to the pumping rate at 35 days is zero. The final condition on λ is designed to ensure that the sensitivity of any performance measure to a parameter arising in future time is rendered zero in (29), consistent with what is evident from physical considerations. Thus, this choice upholds the principle of causality.

$$\lambda(\underline{x},t)\Big|_{t \geq \tau} = 0 \tag{A6}$$

$$[\, S\lambda(\underline{x}\ ,t)\delta p(\underline{x}\ ,t)\ ]_{0}^{\tau} = 0 - S\lambda(\underline{x},0)\delta p(\underline{x},0) \tag{A7}$$

In (A7), for $t = 0$, two cases are examined. Case 1 relates to a purely transient case, for which (3) defines the initial conditions prescribed by the user. They are sensitivity parameters in this context, so that $\delta p(\underline{x},0) = 0$. Case 2 relates to a sequential steady-and-transient analysis, in which pressures given by steady-state analysis constitute the initial conditions for further transient analysis. In such a case, the initial pressures are not parameters but constitute a pressure function evolving from steady-state analysis onto transient-state analysis. Then $\delta p(\underline{x},0) = \delta p_o(\underline{x}) \neq 0$, and the RHS of (A7) reduces to $-S\lambda(\underline{x},0)\ \delta p_o(\underline{x})$. This term would be added to the other terms involving $\delta p_o(\underline{x})$ in the steady state which result from the treatment of terms in $\delta\Omega_o$ (the steady-state counterpart of $\delta\Omega$ in (21)). After simplifications, parallel to those following, $-S\lambda(\underline{x},0)$ would remain as an additional inhomogeneous term in the partial-differential equation for $\lambda_o(\underline{x})$ for the steady state under this option of sequential steady-and-transient analysis [see (38)]. (The physical significance of this term is evident from (66)). Thus,

$$[S\lambda(\underline{x},t)\delta p(\underline{x},t)]_o^{\tau} = 0 \quad ; \quad \text{for Case 1} \tag{A8}$$

$$= -S\lambda(\underline{x},0)\delta p_o(\underline{x}) \; ; \; \text{for Case 2.} \tag{A9}$$

Adding (A4) to the second term of the RHS of (A2) and applying Green's first identity twice to the latter, one has

$$\int_o^{\tau}\int_R -\lambda\nabla\cdot(\rho\delta_p\underline{u})\ d\underline{x}dt + \int_o^{\tau}\int_{\Gamma}\lambda\delta_p\Psi^*\ d\underline{x}dt$$

$$= \int_o^{\tau}[\int_R\lambda\nabla\cdot(\rho\frac{\underline{\underline{k}}}{\mu}\cdot\nabla\lambda)\ \delta p d\underline{x} - \int_{\Gamma}\rho(\frac{\underline{\underline{k}}}{\mu}\cdot\nabla\lambda\cdot\underline{n} + \beta\lambda)\delta p\ d\underline{x}\ ]dt \tag{A10}$$

Using (A5), (A8), and (A10), (A1) may be written as:

$$\int_o^{\tau}\int_R[+S\frac{\partial\lambda}{\partial t} + \nabla\cdot(\rho\frac{\underline{\underline{k}}}{\mu}\cdot\nabla\lambda) + \frac{\partial K}{\partial p}\ ]\ \delta p\ d\underline{x}\ dt$$

$$- \int_{o}^{\tau} \int_{\Gamma} \rho \left(\frac{\underline{\underline{k}}}{\mu} \cdot \nabla\lambda \cdot \underline{n} + \lambda\beta \right) \delta p d\underline{x} \, dt = 0 \tag{A11}$$

If (A11) must hold for arbitrary variations δp, the volume integral and the surface integral must each vanish, leading to:

$$S \frac{\partial \lambda}{\partial t} + \nabla \cdot \left(\rho \frac{\underline{\underline{k}}}{\mu} \cdot \nabla\lambda \right) + \frac{\partial K}{\partial p} = 0 \qquad \text{on } R \times [o, \tau] \tag{A12}$$

$$\frac{\underline{\underline{k}}}{\mu} \cdot \nabla\lambda \cdot \underline{n} + \lambda\beta = 0 \qquad \text{on } \Gamma \times [o, \tau] \tag{A13}$$

Comparison of (A13) and (3) indicates the boundary conditions for λ. Thus, $\lambda = 0$, corresponding to Dirichlet conditions; and $Q_\lambda = 0$ corresponding to Neumann conditions, in the flow problem where

$$Q_\lambda = - \frac{\underline{\underline{k}}}{\mu} \cdot \nabla\lambda \cdot \underline{n} \tag{A14}$$

APPENDIX B: SENSITIVITY COEFFICIENTS OF TRANSIENT-STATE RADIAL FLOW TO A WELL

For transient radial flow around a well pumping at a constant rate in a confined homogeneous isotropic aquifer of constant thickness, Theis (1935) gives:

$$s = \frac{Q}{4\pi\ T} W(u) \tag{B1}$$

where

$$u = \frac{r^2 S^*}{4Tt} \tag{B2}$$

Here Q is constant volumetric pumping rate; T is transmissivity; W is Theis' Well Function for a confined aquifer; S^* is storativity (Dimensionless); t is time since pumping started; s is drawdown of head; and r is radial distance to point of drawdown.

Also,

$$W(u) = \int_u^\infty \frac{e^{-y}}{y} dy \tag{B3}$$

so that,

$$\frac{dW}{du} = \frac{-\ e^{-u}}{u} \tag{B4}$$

Using (B4) and appropriate chain rule of differentiation, one has:

$$\frac{\partial s}{\partial S^*} = (-1) \frac{Q}{4\pi T} \cdot \frac{e^{-u}}{S^*} \tag{B5}$$

$$\frac{\partial s}{\partial T} = \frac{Q}{4\pi T^2} [e^{-u} - W(u)] \tag{B6}$$

$$\frac{\partial s}{\partial Q} = \frac{W(u)}{4\pi T} = \frac{s}{Q} \tag{B7}$$

The following equations relate s, S^*, and T to the variables used in SWIFT II:

$$s = \frac{p(r,0) - p(r,t)}{\rho g} \tag{B8}$$

$$S^* = \phi(C_w + C_r) \rho g b \tag{B9}$$

$$T = \frac{k \rho g b}{\mu} \tag{B10}$$

Using (B8) through (B10), (B5) through (B7) may be recast for application to the SWIFT II and GRASP II codes as:

$$\frac{\partial (p(r,t))}{\partial S^*} = \rho g \frac{Q}{4\pi T} \frac{e^{-u}}{S^*} \tag{B11}$$

$$\frac{\partial p(r,t)}{\partial k} = \frac{b (\rho g)^2 Q}{\mu \quad 4\pi T^2} \{ W(u) - e^{-u} \} \tag{B12}$$

$$\frac{\partial p(r,t)}{\partial Q} = \frac{[p(r,t) - p(r,0)]}{Q} \tag{B13}$$

Here, k is permeability; ρ is density of fluid; g is acceleration due to gravity; b is aquifer thickness; p(r,t) is pressure; C_w is compressibility of water; and C_r is compressibility of rock.

(B11) through (B13) with the definitions in (B9) and (B10) are used for verification of GRASP II in Test Problem 1.

APPENDIX C: SENSITIVITY COEFFICIENTS OF STEADY-STATE CARTESIAN ONE-DIMENSIONAL FLOW

Problem 1

Consider, the one-dimensional steady-state flow through a horizontal heterogeneous aquifer, of length L discretized by N finite-difference grid blocks, subjected to pressure p_o at $x = 0$ and p_L at $x = L$, with $p_o > p_L$ (Figure C.1).

The aquifer may be treated as a network of hydraulic resistors in series (in analogy with electrical resistors), with each grid block represented by one resistor. The hydraulic resistance R_m (the reciprocal of conductance) of grid block m, is given by:

$$R_m = \frac{\Delta x_m \ \mu_m}{k_m \ A_m \ \rho_m} \tag{C1}$$

Here, A is the cross-sectional area of the aquifer normal to x-direction, and other symbols are as defined before. The mass flow rate F through the aquifer is the same at every location, and is given by (using Darcy's law):

$$F = \frac{p_o - p_L}{RT} \tag{C2}$$

$$F = \frac{p_o - p_m}{RL_m} \tag{C3}$$

$$F = \frac{p_m - p_L}{RR_m} \tag{C4}$$

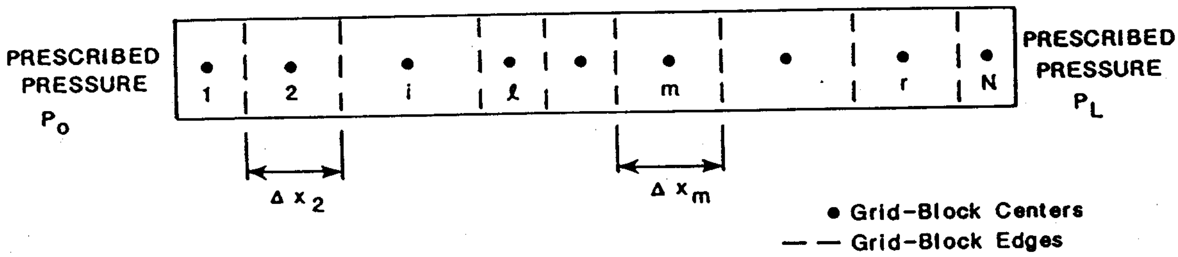

a) Definition Sketch

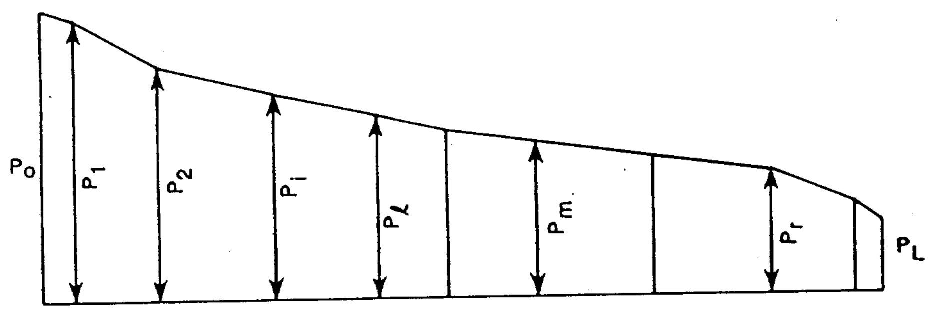

b) Pressure Distribution

Drawn by	Date	One-Dimensional Heterogeneous Aquifer: Problem 1
Checked by	Date	
Revisions	Date	
INTERA Technologies		Figure C.1

Here, RL_m and RR_m are the hydraulic resistances to the left and the right of the grid block m (Figure C.1) and are defined below.

$$RL_m = \sum_{1}^{m-1} R_i + Rm/2 \tag{C5}$$

$$RR_m = \sum_{m+1}^{N} R_i + Rm/2 \tag{C6}$$

$$RT = RL_m + RR_m = \sum_{1}^{N} R_i \tag{C7}$$

The pressure in the center of grid block m, p_m is given by :

$$p_m = [p_o(RR_m) + p_L(RL_m)]/RT \tag{C8}$$

Also, the Darcy flux, u_m, though the grid block is given by

$$u_m = \frac{F_m}{A_m} \tag{C9}$$

Direct differentiation of (C2), (C8), and (C9) provides the sensitivity coefficients for the flux, pressure and Darcy velocity with respect to the desired parameters. However, such sensitivity coefficients for inhomogeneous aquifers are not presented here. Such expressions may then (and only then) be simplified, for a homogeneous aquifer (all k_m are equal) and homogeneous fluid (all ρ_m are equal and all μ_m are equal) discretized by grid blocks of equal length (all Δx_m are equal) giving the following results:

$$\frac{\partial p_m}{\partial k_m} = \frac{1}{2} \frac{(p_o - p_L)}{N} \left[\frac{N-2m+1}{N} \right] \frac{1}{k} \tag{C10}$$

$$\frac{\partial p_m}{\partial k_l} = \frac{(p_o - p_L)}{N} \cdot \frac{(N-m+\frac{1}{2})}{N} \text{ , independent of } l \tag{C11}$$

$$\frac{\partial p_m}{\partial k_r} = \left(\frac{p_o - p_L}{N}\right)\left(\frac{m-\frac{1}{2}}{N}\right)\frac{1}{k} \text{ , independent of } r \tag{C12}$$

(Note : $\sum_{i=1}^{N} \frac{\partial p_m}{\partial k_i} = 0$; as evident from physical considerations)

$$\frac{\partial p_m}{\partial p_o} = (N - m + \tfrac{1}{2})/N \tag{C13}$$

$$\frac{\partial p_m}{\partial p_L} = (m - \tfrac{1}{2})/N \tag{C14}$$

$$\frac{\partial u_m}{\partial k_i} = \frac{u_m}{kN} \tag{C15}$$

$$\frac{\partial u_m}{\partial p_o} = \frac{u_m}{(p_o - p_L)} \tag{C16}$$

Problem 2

Consider a one-dimensional aquifer, just as in Problem 1, but with different boundary conditions, viz. zero pressures prescribed at x=0, and x = L. A fluid source of strength q_m (mass rate) is introduced into the grid block m. The mass flow rate q_m gets divided into q_l towards the left and q_r towards the right of the grid block m shown in Figure C.2. Let p_m be the pressure at the center of grid block m.

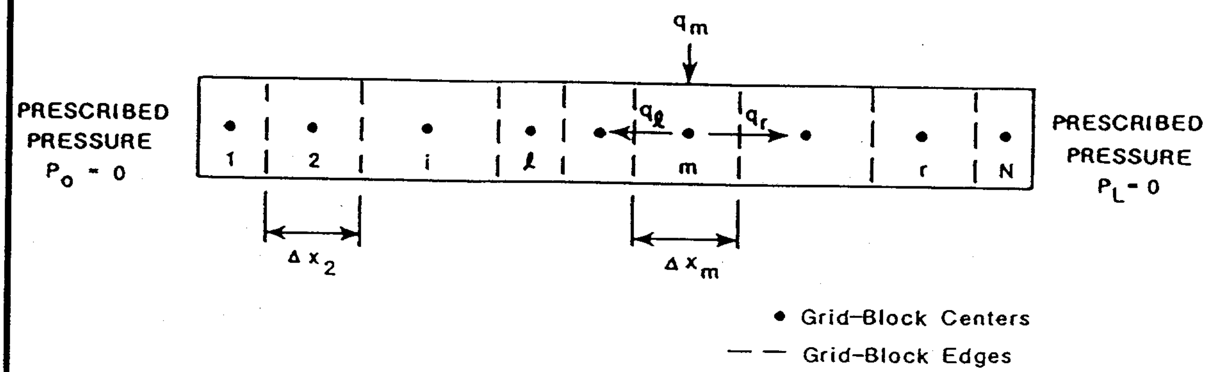

a) Definition Sketch

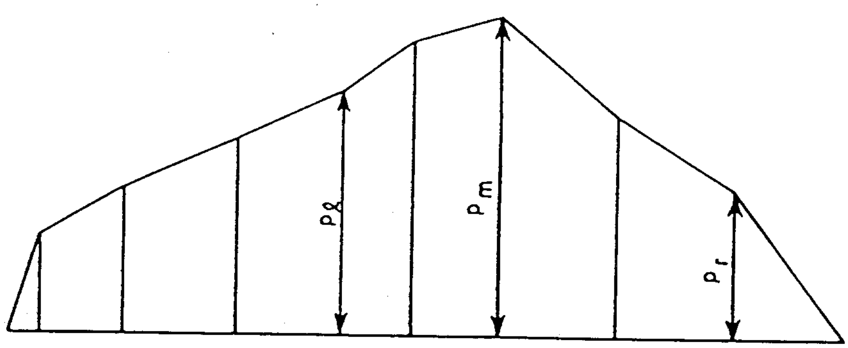

b) Pressure Distribution

Drawn by	Date
Checked by	Date
Revisions	Date

One–Dimensional Heterogeneous Aquifer: Problem 2

INTERA Technologies

Figure C.2

$$q_l = \frac{p_m - 0}{RL_m} \quad , \tag{C17}$$

$$q_r = \frac{p_m - 0}{RR_m} \tag{C18}$$

$$q_m = q_l + q_r = \quad p_m \left[\frac{1}{RL_m} + \frac{1}{RR_m}\right] \tag{C19}$$

where RL_m and RR_m are as defined in (C5) and (C6).

$$p_m = \frac{q_m \, RR_m \, RL_m}{RT} \tag{C20}$$

$$\begin{aligned} p_l &= q_l \, RL_l \\ &= \frac{q_m \, RR_m \, RL_l}{RT} \end{aligned} \tag{C21}$$

$$p_r = \frac{q_m \, RL_m \, RR_r}{RT} \tag{C22}$$

Here, p_l and p_r are the pressures in the grid-blocks l and r respectively. Also, RL and RR refer to the hydraulic resistances to the left and the right of a grid block indicated by the suffix, such as l, r, or m (Figure C.2).

$$u_l = \frac{q_l}{\rho_l Al} \tag{C23}$$

$$u_r = \frac{q_r}{\rho_r A_r} \tag{C24}$$

Here, u_l and u_r are Darcy fluxes in the grid-blocks l and r respectively.

In Problem 1, p_m does not depend upon q. So superimpose the results of the Problems 1 and 2. Then performing the differentiation with q_m and then setting q_m to zero (not needed here) gives the sensitivity coefficients for the parameter q_m. These sensitivity coefficients constitute the adjoint states. Then, (and only then) simplifying the results to the case of homogeneous aquifer and fluid, with equal lengths of grid blocks, one obtains:

$$\frac{\partial p_m}{\partial q_m} = \frac{(N-m+\frac{1}{2})\ (m-\frac{1}{2})}{N} \frac{\Delta x}{kA} \frac{\mu}{\rho} \tag{C25}$$

$$\frac{\partial p_l}{\partial q_m} = \frac{(N-m+\frac{1}{2})\ (l-\frac{1}{2})}{N} \frac{\Delta x}{kA} \frac{\mu}{\rho} \tag{C26}$$

$$\frac{\partial p_r}{\partial q_m} = \frac{(m-\frac{1}{2})\ (N-r+\frac{1}{2})}{N} \frac{\Delta x}{kA} \frac{\mu}{\rho} \tag{C27}$$

$$\frac{\partial u_r}{\partial q_m} = \frac{(m-\frac{1}{2})}{N} \frac{1}{A\rho} \tag{C28}$$

$$\frac{\partial u_l}{\partial q_m} = \frac{(N-m+\frac{1}{2})}{N} \frac{1}{A\rho} \tag{C29}$$

$$\frac{\partial u_m}{\partial q_m} = \frac{(2m-1-N)}{N} \frac{1}{A\rho} \tag{C30}$$

FEDERAL AGENCIES

U. S. Department of Energy, (5)
Office of Civilian Radioactive Waste
  Management
Attn: Deputy Director, RW-2
  Associate Director, RW-10
    Office of Program Administration
     and Resources Management
  Associate Director, RW-20
    Office of Facilities Siting
     and Development
  Associate Director, RW-30
    Office of Systems Integration
     and Regulations
  Associate Director, RW-40
    Office of External Relations
     and Policy
Forrestal Building
Washington, DC 20585

U. S. Department of Energy (3)
Albuquerque Operations Office
Attn: J. E. Bickel
  R. Marquez, Director
   Public Affairs Division
P.O. Box 5400
Albuquerque, NM 87185

U. S. Department of Energy
Attn: National Atomic Museum Library
Albuquerque Operations Office
P. O. Box 5400
Albuquerque, NM 87185

U. S. Department of Energy (9)
WIPP Project Office (Carlsbad)
Attn: A. Hunt (4)
  V. Daub (2)
  J. A. Mewhinney
  R. Batra
  J. Carr
P.O. Box 3090
Carlsbad, NM 88221

U. S. Department of Energy
Research & Waste Management Division
Attn: Director
P. O. Box E
Oak Ridge, TN 37831

U.S. Department of Energy
Richland Operations Office
Nuclear Fuel Cycle & Production
Division
Attn: R. E. Gerton
P.O. Box 500
Richland, WA 99352

U. S. Department of Energy (1)
Attn: Edward Young
Room E-178
GAO/RCED/GTN
Washington, DC 20545

U. S. Department of Energy (6)
Office of Environmental Restoration
and Waste Management
Attn: Jill Lytle, EM30
Mark Frei, EM-34 (3)
Mark Duff, EM-34
Clyde Frank, EM-50
Washington, DC 20585

U. S. Department of Energy (3)
Office of Environment, Safety
and Health
Attn: Ray Pelletier, EH-231
Kathleen Taimi, EH-232
Carol Borgstrom, EH-25
Washington, DC 20585

U. S. Department of Energy (2)
Idaho Operations Office
Fuel Processing and Waste
Management Division
785 DOE Place
Idaho Falls, ID 83402

U.S. Department of Energy
Savannah River Operations Office
Defense Waste Processing
Facility Project Office
Attn: W. D. Pearson
P.O. Box A
Aiken, SC 29802

U.S. Environmental Protection Agency (2)
Attn: Ray Clark
Office of Radiation Programs (ANR-460)
Washington, DC 20460

U.S. Geological Survey
Branch of Regional Geology
Attn: R. Snyder
MS913, Box 25046
Denver Federal Center
Denver, CO 80225

U.S. Geological Survey
Conservation Division
Attn: W. Melton
P.O. Box 1857
Roswell, NM 88201

U.S. Geological Survey (1)
Water Resources Division
Attn: Kathy Peter
Suite 200
4501 Indian School, NE
Albuquerque, NM 87110

U.S. Nuclear Regulatory Commission (4)
Attn: Joseph Bunting, HLEN 4H3 OWFN
Ron Ballard, HLGP 4H3 OWFN
Jacob Philip
NRC Library
Mail Stop 623SS
Washington, DC 20555

Boards

Defense Nuclear Facilities Safety Board
Attn: Dermot Winters
Suite 675
600 E Street, NW
Washington, DC 20004

U. S. Department of Energy
Advisory Committee on Nuclear
Facility Safety
Attn: Merritt E. Langston, AC21
Washington, DC 20585

Nuclear Waste Technical
Review Board (2)
Attn: Dr. Don A. Deere
Dr. Sidney J. S. Parry
Suite 910
1100 Wilson Blvd.
Arlington, VA 22209-2297

Richard Major
Advisory Committee
on Nuclear Waste
Nuclear Regulatory Commission
7920 Norfolk Avenue
Bethesda, MD 20814

George M. Hornberger
Board on Radioactive Waste Management
Department of Environmental Engineering
Clark Hall
University of Virginia
Charlottesville, VA 22903

STATE AGENCIES

Environmental Evaluation Group (3)
Attn: Library
Suite F-2
7007 Wyoming Blvd., N.E.
Albuquerque, NM 87109

New Mexico Bureau of Mines
and Mineral Resources (2)
Attn: F. E. Kottolowski, Director
J. Hawley
Socorro, NM 87801

NM Department of Energy & Minerals
Attn: Librarian
2040 S. Pacheco
Santa Fe, NM 87505

NM Environmental Improvement Division
Attn: Deputy Director
1190 St. Francis Drive
Santa Fe, NM 87503

LABORATORIES/CORPORATIONS

Battelle Pacific Northwest Laboratories (6)
Attn: D. J. Bradley, K6-24
J. Relyea, H4-54
R. E. Westerman, P8-37
S. Bates, K2-57
H. C. Burkholder, P7-41
L. Pederson, K6-47
Battelle Boulevard
Richland, WA 99352

Savannah River Laboratory (6)
Attn: N. Bibler
E. L. Albenisius
M. J. Plodinec
G. G. Wicks
C. Jantzen
J. A. Stone
Aiken, SC 29801

George Dymmel
SAIC
101 Convention Center Dr.
Las Vegas, NV 89109

INTERA Inc. (9)
Attn: G. E. Grisak
J. F. Pickens (7)
A. Haug
Suite #300
6850 Austin Center Blvd.
Austin, TX 78731

INTERA Inc. (3)
Attn: Wayne Stensrud
P.O. Box 2123
Carlsbad, NM 88221

INTERA Inc. (3)
Attn: Marsh LaVenue
8100 Mountain Road
Suite #204D
Albuquerque, NM 87110

IT Corporation (4)
Attn: R. F. McKinney
J. Myers
P. Drez
H. Dove
Regional Office - Suite 700
5301 Central Avenue, NE
Albuquerque, NM 87108

IT Corporation (2)
Attn: D. E. Deal
P.O. Box 2078
Carlsbad, NM 88221

Charles R. Hadlock
Arthur D. Little, Inc.
Acorn Park
Cambridge, MA 02140-2390

Los Alamos Scientific Laboratory
Attn: B. Erdal, CNC-11
Los Alamos, NM 87545

Oak Ridge National Laboratory (4)
Attn: T. F. Lomenick
Box 2009
Oak Ridge, TN 37831

RE/SPEC, Inc. (3)
Attn: W. Coons
P. F. Gnirk
M. Wallace
P.O. Box 14984
Albuquerque NM 87191

RE/SPEC, Inc. (7)
Attn: L. L. Van Sambeek
G. Callahan
T. Pfeifle
J. L. Ratigan
P. O. Box 725
Rapid City, SD 57709

Center for Nuclear Waste
Regulatory Analysis (4)
Attn: P. K. Nair
Southwest Research Institute
6220 Culebra Road
San Antonio, TX 78228-0510

Science Applications
International Corporation
Attn: Howard R. Pratt,
Senior Vice President
10260 Campus Point Drive
San Diego, CA 92121

Science Applications
International Corporation
Attn: Michael B. Gross
Ass't. Vice President
Suite 1250
160 Spear Street
San Francisco, CA 94105

Systems, Science, and Software (2)
Attn: E. Peterson
P. Lagus
Box 1620
La Jolla, CA 92038

Westinghouse Electric Corporation (7)
Attn: Library
Lamar Trego
W. P. Poirer
W. R. Chiquelin
V. F.Likar
D. J. Moak
R. F. Kehrman
P. O. Box 2078
Carlsbad, NM 88221

Weston Corporation (1)
Attn: David Lechel
Suite 1000
5301 Central Avenue, NE
Albuquerque, NM 87108

Durham Geological Association
908 Town & Country Blvd.
Suite 120
Houston, TX 77024

GRAM, Inc.
Attn: D. A. Zimmerman
1709 Moon NE
Albuquerque, NM 87111

UNIVERSITIES

University of Arizona
Attn: J. G. McCray
Department of Nuclear Engineering
Tucson, AZ 85721

University of New Mexico (2)
Geology Department
Attn: D. G. Brookins
Library
Albuquerque, NM 87131

Pennsylvania State University
Materials Research Laboratory
Attn: Della Roy
University Park, PA 16802

Texas A&M University (4)
Center of Tectonophysics
Attn: R. Carlson
B. Johnson
J. Russell
E. Hoskins
College Station, TX 77840

Texas A&M University
Department of Geology
Attn: P. A. Domenico
College Station, TX 77840

New Mexico Tech (3)
Department of Geoscience
Attn: J. Wilson
A. Gutjahr
F. Phillips
Socorro, NM 87801

G. Ross Heath
College of Ocean
and Fishery Sciences
University of Washington
Seattle, WA 98195

INDIVIDUALS

Dennis W. Powers
Star Route Box 87
Anthony, TX 79821

LIBRARIES

Thomas Brannigan Library
Attn: Don Dresp, Head Librarian
106 W. Hadley St.
Las Cruces, NM 88001

Hobbs Public Library
Attn: Ms. Marcia Lewis, Librarian
509 N. Ship Street
Hobbs, NM 88248

New Mexico State Library
Attn: Ms. Ingrid Vollenhofer
P.O. Box 1629
Santa Fe, NM 87503

New Mexico Tech
Martin Speere Memorial Library
Campus Street
Socorro, NM 87810

Pannell Library
Attn: Ms. Ruth Hill
New Mexico Junior College
Lovington Highway
Hobbs, NM 88240

WIPP Public Reading Room
Attn: Director
Carlsbad Public Library
101 S. Halagueno St.
Carlsbad, NM 88220

Government Publications Department
General Library
University of New Mexico
Albuquerque, NM 87131

THE SECRETARY'S BLUE RIBBON PANEL ON WIPP

Dr. Thomas Bahr
New Mexico Water Resources Institute
New Mexico State University
Box 3167
Las Cruces, NM 88003-3167

Mr. Leonard Slosky
Slosky and Associates
Suite 1400
Bank Western Tower
1675 Tower
Denver, Colorado 80202

Mr. Newal Squyres
Eberle and Berlin
P. O. Box 1368
Boise, Idaho 83701

Dr. Arthur Kubo
Vice President
BDM International, Inc.
7915 Jones Branch Drive
McLean, VA 22102

Mr. Robert Bishop
Nuclear Management Resources Council
Suite 300
1776 I Street, NW
Washington, DC 20006-2496

NATIONAL ACADEMY OF SCIENCES, WIPP PANEL

Dr. Charles Fairhurst, Chairman
Department of Civil and
Mineral Engineering
University of Minnesota
500 Pillsbury Dr. SE
Minneapolis, MN 55455

Dr. John O. Blomeke
Route 3
Sandy Shore Drive
Lenoir City, TN 37771

Dr. John D. Bredehoeft
Western Region Hydrologist
Water Resources Division
U.S. Geological Survey (M/S 439)
345 Middlefield Road
Menlo Park, CA 94025

Dr. Karl P. Cohen
928 N. California Avenue
Palo Alto, CA 94303

Dr. Fred M. Ernsberger
250 Old Mill Road
Pittsburgh, PA 15238

Dr. Rodney C. Ewing
Department of Geology
University of New Mexico
200 Yale, NE
Albuquerque, NM 87131

B. John Garrick
Pickard, Lowe & Garrick, Inc.
2260 University Drive
Newport Beach, CA 92660

John W. Healy
51 Grand Canyon Drive
Los Alamos, NM 87544

Leonard F. Konikow
U.S. Geological Survey
431 National Center
Reston, VA 22092

Jeremiah O'Driscoll
505 Valley Hill Drive
Atlanta, GA 30350

Dr. Christopher G. Whipple
Electric Power Research Institute
3412 Hillview Avenue
Palo Alto, CA 94303

Dr. Peter B. Myers, Staff
Director
National Academy of Sciences
Committee on Radioactive
Waste Management
2101 Constitution Avenue
Washington, DC 20418

Dr. Geraldine Grubb
Board on Radioactive
Waste Management
GF462
2101 Constitution Avenue
Washington, DC 20418

FOREIGN ADDRESSES

Studiecentrum Voor Kernenergie
Centre D'Energie Nucleaire
Attn: Mr. A. Bonne
SCK/CEN
Boeretang 200
B-2400 Mol
BELGIUM

Atomic Energy of Canada, Ltd. (2)
Whiteshell Research Estab.
Attn: Peter Haywood
John Tait
Pinewa, Manitoba, CANADA
R0E 1L0

Dr. D. K. Mukerjee
Ontario Hydro Research Lab
800 Kipling Avenue
Toronto, Ontario, CANADA
M8Z 5S4

Mr. Francois Chenevier, Director (2)
ANDRA
Route du Panorama Robert Schumann
B.P.38
92266 Fontenay-aux-Roses Cedex
FRANCE

Mr. Jean-Pierre Olivier
OECD Nuclear Energy Agency
Division of Radiation Protection
and Waste Management
38, Boulevard Suchet
75016 Paris, FRANCE

Claude Sombret
Centre D'Etudes Nucleaires
De La Vallee Rhone
CEN/VALRHO
S.D.H.A. BP 171
30205 Bagnols-Sur-Ceze
FRANCE

Bundesministerium fur Forschung und
Technologie
Postfach 200 706
5300 Bonn 2
FEDERAL REPUBLIC OF GERMANY

Bundesanstalt fur Geowissenschaften
und Rohstoffe
Attn: Michael Langer
Klaus Schelkes
Postfach 510 153
3000 Hannover 51
FEDERAL REPUBLIC OF GERMANY

Gesellschaft fur Reaktorsicherheit
Attn: Peter Bogorinski
Schwertnergasse 1
5000 Koln 1
FEDERAL REPUBLIC OF GERMANY

Gesellschaft fur Strahlen-und Umweltforschung mbH
Attn: Richard Storck
Theodor-Heuss-Str. 4
D-3300 Braunschweig
FEDERAL REPUBLIC OF GERMANY

Hahn-Meitner-Institut fur Kernforschung
Attn: Werner Lutze
Glienicker Strasse 100
100 Berlin 39
FEDERAL REPUBLIC OF GERMANY

Institut fur Tieflagerung (4)
Attn: K. Kuhn
Theodor-Heuss-Strasse 4
D-3300 Braunschweig
FEDERAL REPUPLIC OF GERMANY

Kernforschug Karlsruhe
Attn: K. D. Closs
Postfach 3640
7500 Karlsruhe
FEDERAL REPUBLIC OF GERMANY

Physikalisch-Technische Bundesanstalt
Attn: Peter Brenneke
Postfach 33 45
D-3300 Braunschweig
FEDERAL REPUBLIC OF GERMANY

D. R. Knowles
British Nuclear Fuels, plc
Risley, Warrington, Cheshire WA3 6AS
1002607 GREAT BRITAIN

Shingo Tashiro
Japan Atomic Energy Research Institute
Tokai-Mura, Ibaraki-Ken
319-11 JAPAN

Netherlands Energy Research Foundation
ECN (2)
Attn: Tuen Deboer, Mgr.
L. H. Vons
3 Westerduinweg
P.O. Box 1
1755 ZG Petten
THE NETHERLANDS

Rijksinstituut Voor Volksgezondheid en Milieuhygiene (RIVM) (2)
Attn: Peter Glasbergen
Seyed M. Hassanizandeh
P. O. Box 1
3720 BA Bilthoven
THE NETHERLANDS

Svensk Karnbransleforsorjning AB
Attn: Fred Karlsson
Project KBS
Karnbranslesakerhet
Box 5864
10248 Stockholm
SWEDEN

NAGRA
Attn: Stratis Vomvoris
Parkstr. 23
CH-5401 Baden
SWITZERLAND

COLENCO
Attn: Olivier Jaquet
Parkstr. 27
CH-5401 Baden
SWITZERLAND

SANDIA INTERNAL

400	L. D. Tyler
1510	J. W. Nunziato
1520	C. W. Peterson
1521	J. G. Arguello
1521	H. S. Morgan
3141	S. A. Landenberger (5)
3141-1	C. L. Ward, (8) for DOE/OSTI
3151	Supervisor (3)
6000	V. L. Dugan, Acting
6232	W. R. Wawersik
6233	J. C. Eichelberger
6233	J. L. Krumhansl
6300	T. O. Hunter, Acting
6310	T. E. Blejwas, Acting
6313	T. Blejwas
6340	W. D. Weart
6340	S. Y. Pickering
6341	R. C. Lincoln
6341	Staff (7)
6341	Sandia WIPP Central Files (10)
6342	D. R. Anderson
6342	Staff (11)
6343	T. M. Schultheis
6343	Staff (2)
6344	E. Gorham
6344	Staff (8)
6344	P. B. Davies (7)
6344	M. LaVenue
6345	A. R. Lappin
6345	Staff (9)
6346	J. R. Tillerson
6346	Staff (7)
6350	W. C. Luth
6416	E. J. Bonano
6416	J. McCord
6416	S. Conrad
7223	C. Gotway
8524	J. A. Wackerly (SNLL Library)
9300	J. E. Powell
9310	J. D. Plimpton
9320	M. J. Navratil
9325	R. L. Rutter
9325	J. T. McIlmoyle
9330	J. D. Kennedy
9333	O. Burchett
9333	J. W. Mercer
9334	P. D. Seward

*U.S. GOVERNMENT PRINTING OFFICE 1990-0-573-038/20027

8232-2/070987

00000001 -

8232-2/070987

00000001 -

8232-2/070987

00000001 -

8524
8524-2